Quaternary Science Reviews 272 (2021) 107199

Contents lists available at ScienceDirect

Quaternary Science Reviews

journal homepage: www.elsevier.com/locate/quascirev

Environmental changes in the late Allerød and early Younger Dryas in the Netherlands: a multiproxy high-resolution record from a site with two *Pinus sylvestris* populations

Jos Bazelmans [a, *], Ronald van Balen [b, j], Johanna Bos [c], Otto Brinkkemper [a], Jesper Colenberg [d], Petra Doeve [e], Bas van Geel [f], Tom Hakbijl [g], Hans van Hateren [b], Wim Z. Hoek [h], Hans Huisman [a], Esther Jansma [a, e], Cornelis Kasse [b], Bertil van Os [a], Hans van der Plicht [i], Jeroen Schokker [j], Nathalie Van der Putten [b], John van der Woude [b]

[a] *Cultural Heritage Agency of the Netherlands, Smallepad 5, 3811 MG Amersfoort, the Netherlands*
[b] *Earth Sciences, Vrije Universiteit, De Boelelaan 1105, 1081 HV Amsterdam, the Netherlands*
[c] *ADC Archeoprojecten, Nijverheidsweg-Noord 114, 3812 PN Amersfoort, the Netherlands*
[d] *MiArch, Botter 41-17, 8243 KZ Lelystad, the Netherlands*
[e] *Netherlands Centre for Dendrochronology/RING Foundation, Smallepad 5, 3811 MG Amersfoort, the Netherlands*
[f] *Institute for Biodiversity and Ecosystem Dynamics, University of Amsterdam, Science Park 904, 1098 XH Amsterdam, the Netherlands*
[g] *Naturalis Biodiversity Centre, Darwinweg 2, 2333 CR Leiden, the Netherlands*
[h] *Department of Physical Geography, Utrecht University, Princetonlaan 4, 3584 CB Utrecht, the Netherlands*
[i] *Centre for Isotope Research, Groningen University, Nijenborgh 6, 9747 AG Groningen, the Netherlands*
[j] *TNO, Geological Survey of the Netherlands, Princetonlaan 6, 3584 CB Utrecht, the Netherlands*

ARTICLE INFO

Article history:
Received 8 July 2021
Received in revised form
17 September 2021
Accepted 17 September 2021
Available online xxx

Handling Editor: Dr A. Voelker

Keywords:
Allerød
Younger Dryas event
Climate change
Pinus sylvestris
In situ Late Glacial tree remains
Waterlogged Usselo or Finow soil
Dendrochronology
Multiproxy analysis

ABSTRACT

In the Netherlands, several proxies of climate change during the Last Glacial-Interglacial Transition (LGIT) (c. 14,700 to 11,700 b2k) have been investigated in detail over the last few decades. The present paper presents two tree-ring chronologies LETR-A (n = 16, timespan 106 rings) and LETR-B (n = 24, timespan 201 rings) from *in situ* subfossil pine remains (*Pinus sylvestris*) discovered at Leusden-Den Treek in the Netherlands that date from the Bølling-Allerød interstadial (GI-1). Using a multiproxy approach (both abiotic and biotic), it was possible to study local woodland development in detail as part of long-term environmental change. Moreover, the trees opened up possibilities for dendrochronological and dendroclimatological research. The tree-ring series show the occurrence of two successive phases of pine woodland development, which were ^{14}C dated with high precision and calibrated using the recent IntCal20 ^{14}C calibration curve: 13,450–13,396 to 13,370–13,316 calBP (series LETR-A) and 12,952–12,937 to 12,754–12,739 calBP (series LETR-B). At the north-western boundary of its ecotone, *Pinus* was highly sensitive to climate change during the latter part of GI-1 and the transition to GS-1. The inability to set fruit and the disappearance of the pine woodland within decades before and after c. 12,745 calBP is interpreted as the vegetational response to abrupt climate deterioration at the start of the Younger Dryas (12,807 ± 12 cal BP).

1. Introduction

The Last Glacial-Interglacial Transition (LGIT), c. 14,700 to 11,700 b2k, marks the transition from the cold Weichselian Late-Glacial to the warm Holocene (Hoek, 2008)(throughout this paper b2k dates are used if based on the INTIMATE Event Stratigraphy, i.e. calender years relative to 2000 CE. Dates based on ^{14}C analysis are reported in calBP, i.e. calender years relative to 1950 CE). The LGIT was a time period with marked climate variability and subsequent environmental change (Rasmussen et al., 2006, 2014; Lowe et al., 2008). At times within the LGIT, climate change was abrupt and intense. A canonical example for the northern hemisphere is the Younger Dryas cooling event, comparable to GS-1 (~12,900–11,700 b2k)

* Corresponding author. Cultural Heritage Agency, P.O. Box 1600, 3800, BP, Amersfoort, the Netherlands.
E-mail address: j.bazelmans@cultureelerfgoed.nl (J. Bazelmans).

https://doi.org/10.1016/j.quascirev.2021.107199

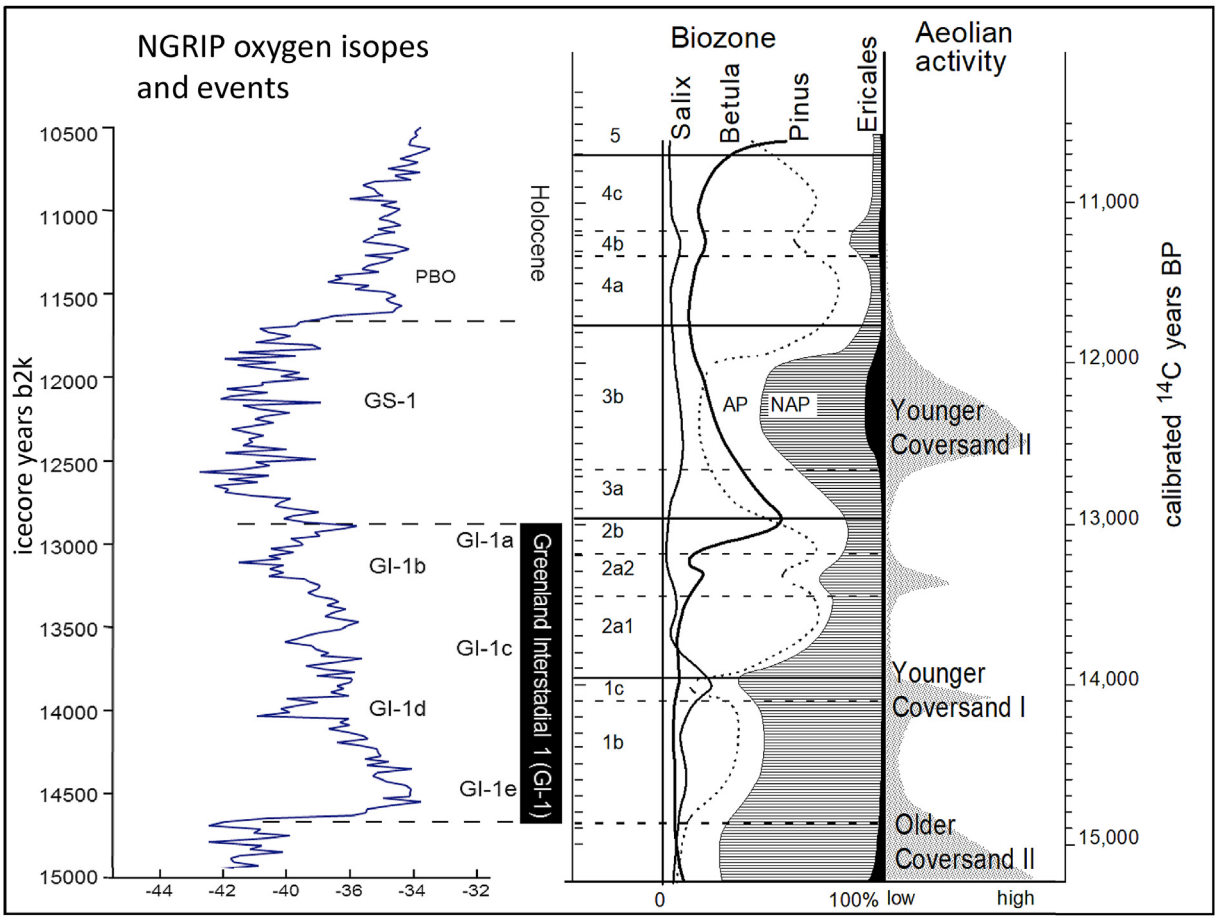

Fig. 1. Schematic overview of Late-Glacial vegetational and aeolian events in the Netherlands compared to the INTIMATE Event Stratigraphy with the Greenland Interstadial GI-1 and sub-events and Greenland Stadial GS-1 plotted against the GICC05 age in years b2k (after Rasmussen et al., 2014). Vegetation events based on pollen records from the Netherlands plotted against a calibrated ^{14}C timescale represent biozones corresponding to the warmer Bølling (zone 1b) and Allerød (zone 2) as well as the colder Younger Dryas (zone 3) periods (after Hoek, 2001; Hoek and Bohncke, 2002). The more open vegetation phases with high percentages of non-arboreal pollen (NAP) correspond to phases of increased aeolian activity, particularly during the Older Dryas (zone 1c), intra-Allerød cold period (zone 2a2), and second phase of Younger Dryas (zone 3b). Overall, a correlation between warmer phases in the NGRIP record and the percentage of arboreal pollen (AP) can be seen, with the development of pine woodland during the later part of the Allerød (zone 2b).

(Brauer et al., 2008; Carlson, 2013; Rea et al., 2020; Renssen, 2020; Mangerud, 2021). Within the Late-Glacial Interstadial (comparable to GI-1), several smaller warmer and cooler phases can be identified (Steffensen et al., 2008). To investigate the nature of LGIT climate change in high resolution, abiotic and biotic evidence can be converted into quantified climate parameter values using standardized (mathematical) translations (Vandenberghe et al., 1998; Moreno et al., 2014). Subsequent time lags in the response by different proxies and geographical time lags in climate change need to be researched (Lane et al., 2013). For Mangerud (2021) 'such discussions of time lags must be performed by comparing ages directly in years for changes at different sites, or relative to volcanic ash beds, or as stratigraphically different responses of proxies in the same section or core'. In the Netherlands, several records of LGIT climate change have been investigated in that way in detail over the last few decades (Van Geel et al., 1989; Hoek, 1997; Hoek and Bohncke, 2002; Van Asch et al., 2013) (Fig. 1). In most cases, however, a precise dating is not possible for various methodological reasons. To overcome this, this paper presents a high resolution multi-proxy study of a waterlogged paleosol of Allerød age (i.e. Usselo or Finow soil, Hijszeler, 1957; Van der Hammen, 1951; Kaiser et al., 2009; Van Hoesel et al., 2012, Vandenberghe et al., 2013) from the Den Treek estate at Leusden, the Netherlands. Here, a large number of *in situ* Allerød subfossil *Pinus* trees (n = 165) were found and documented. Trees from the Last Glacial-Interglacial Transition are rare in Europe (Friedrich et al., 2004; Kaiser et al., 2012, 2018; Dzieduszyńska et al., 2014; Capano et al., 2018; Reinig et al., 2018). They are important for creating continuous tree-ring chronologies and hence for the study of variation in ^{14}C in the atmosphere (Reinig et al., 2020). However, their use for LGIT climate reconstruction is underexplored and difficult (Pauly et al., 2020). For the Leusden woodland it was possible to build a radiocarbon dated tree-ring chronology for two successive pine woodland stands from the site. In addition, years or prolonged periods of reduced tree growth were identified for both stands. It was possible to interpret local environmental changes and pine woodland development in relationship to the LGIT event stratigraphy and the onset of the Younger Dryas (Lowe et al., 2008; Rasmussen et al., 2014; Reinig et al., 2021).

2. Methods

2.1. Study site

Leusden-Den Treek (WGS 84 coordinates: N52° 07.207′, E005° 22.816'; National Triangulation System (RD) coordinates:

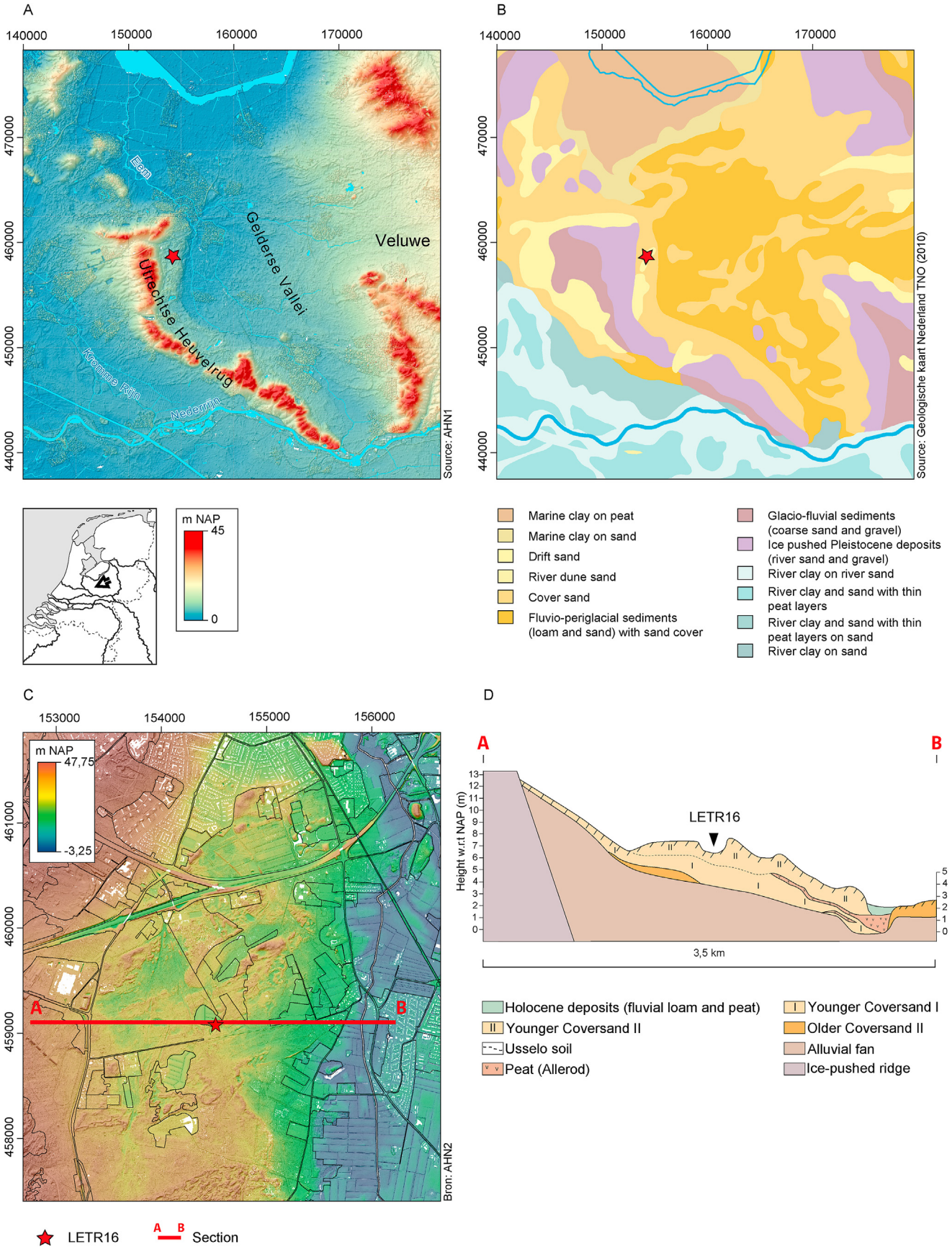

Fig. 2. Location of the Leusden-Den Treek study site. A) Lidar image of the glacial tongue basin of the *Gelderse Vallei* and the ice pushed ridges of the *Utrechtse Heuvelrug* and the *Veluwe* (MIS 6) in the central Netherlands. B) Geological setting. C) Lidar image of the study site with geological cross section AB. D) Simplified geological cross section AB (Westerink, 1981). National Triangulation System (RD) in m.

154,525 × 459,100 m) is situated at the eastern slope of the *Utrechtse Heuvelrug*, a heavily eroded Saalian (MIS 6) sand and gravel ice-pushed ridge (Fig. 2A). The site is located at 7 m + NAP (throughout this paper *Normaal Amsterdam Peil* (NAP) or Amsterdam Ordnance Datum is used as a vertical datum), at the western edge of the former Amersfoort glacial basin in an approximately 25 km long and 3 km wide belt of Weichselian Late Pleniglacial and Late-Glacial coversand (i.e. Boxtel Formation, Wierden Member) (Kasse, 1999, 2002; Schokker et al., 2007; Van Balen et al., 2019) (Fig. 2B). Underneath Younger Coversand II of Younger Dryas age and on top of Older Coversand and Younger Coversand I (Kasse et al., 2007; Vandenberghe et al., 2013; Kasse et al., 2018), a paleosol from the Allerød (Usselo or Finow paleosol) has been found at Leusden and in many other places within these sands (Florschütz, 1941; Van der Hammen, 1951; Maarleveld and van der Schans, 1961; De Jong, 1979; Westerink, 1981; Van Mourik and Slotboom, 1995) (Fig. 2C and Fig. 2D). Buried Usselo paleosols are found within the northern and central European sand belt and are typically 5–30 cm thick (Kaiser et al., 2009). They are frequently characterized by pieces of *Pinus* charcoal, mottling due to bioturbation and burrowing by dung beetles (Van Hoesel et al., 2012; Vandenberghe et al., 2013). Numerous palynological studies indicate the presence of pine woodland based on high percentages of *Pinus* pollen during the second part of the Allerød (Hoek, 1997). However, apart from a concise paper on the occurrence of pine tree remains near Helvoirt (Polak, 1963), the mentioning in passing of partially carbonized trunks of pines and birch at Usselo (Van der Hammen, 1951) and the occurrence of macrofossils of *Pinus sylvestris* (Van Geel et al., 1989; Bohncke, 1993; Bos et al., 2006), the literature contains no indications of the existence of remains of Allerød subfossil pine woodland found in the Netherlands.

The Leusden trees were excavated in a wet depression of 35,000 m^2 which was drained in the late 18th century and used thereafter as pasture. The area still clearly contained recoverable quantities of Holocene peat after drainage (Perks, 1984). That peat deposit has since disappeared through human extraction (for use as fuel) and oxidation. Degradation of the overlying peat created a centimetres-thick dark reddish-brown humus illuviation horizon just above the Usselo soil (i.e. iron pan or 'waterhard' layer; Dekker et al., 1991; Koopman, 1986; Koopman, 1988) and the illuviation, as was established during fieldwork, of a brownish-black humous jelly consisting of Ca-humic complexes (i.e. dopplerite) (Gregorich et al., 2001; Nijland et al., 2007; Van Heuveln and De Bakker, 1972) on, around and below the *Pinus* trees. A thin plough layer now lies directly on top of the coversand.

2.2. Fieldwork

Subfossil woodland remains were found by chance in the summer of 2016 during sand-extraction operations (Fig. 3A). Based on the stratigraphic position of the trees in or on a partly cryoturbated waterlogged Usselo soil and taking into account common knowledge of the vegetation history of the Late-Glacial period, it was evident that the remains date from the later part of the Bølling-Allerød interstadial. The absolute height levels of the Usselo soil within the sand extraction area show that the landscape in the late Allerød was slightly undulating. An Usselo soil is absent in the western part of the sand extraction area. In the eastern part it is present between 5.35 and 6.70 m + NAP. However, subfossil woodland remains are only preserved in the southeastern corner of the sand extraction area, in places where the Usselo soil is below 5.50 m + NAP and permanently waterlogged.

It was possible to excavate the site during four short fieldwork campaigns, numbering twelve days in total, between July 2016 and January 2017 (Cultural Heritage Agency project code LETR16). Only a small portion of the woodland remains within the sand extraction area was lost unseen. Immediately prior to the commercial sand extraction, a digger was used to remove approx. 1.5 m of coversand and an excavation level was created in the top of the Usselo soil (Fig. 3B). The stumps and fallen trees were uncovered using shovels and trowels, and prior to sampling their dimensions and position were measured in 3D with 1 cm precision using a robotic total station (Fig. 3C). In total, six excavation trenches were dug (Fig. 4). Within a total area of 2,700 m^2, 165 pine trees (*Pinus sylvestris*) and two birch trees (*Betula* sp.) were documented and sampled for dendrochronological analysis (where possible ca 1 m above the stump), in some cases resulting in multiple samples per tree (total number of samples: 181). To obtain a picture of the geological, pedological and palaeoecological context of the trees, a profile was established across the site at the south side of trench 5, which was then studied, photographed, drawn and sampled (Figs. 3B, 4 and 5 (profile AD and subprofile BC with samples LETR16-128, 129, 222 and 223). Within the excavation several additional soil samples were taken. Two of them were used for further analysis and are discussed below: LETR16-5 and LETR16-69 (Fig. 4 with samples LETR16-5 in trench 3 and LETR16-69 in trench 4).

2.3. Sampling

A lithostratigraphic description of subprofile BC (Fig. 5A and Fig. 5B) was combined with samples (i.e. sequences) of the same profile for micromorphological (LETR16-129), handheld XRF (LETR16-129) and grain size (LETR16-128) analysis (see below for sample nature and size). Two samples from subprofile CD were used for pollen analysis (LETR16-222 and LETR16-223). One sample was taken from the western profile of excavation trench 1 (LETR16-5) for more extensive sedimentological analysis and one sample from a profile within excavation trench 3 (LETR16-69) for more extensive palaeoecological analysis. The stratigraphy at the sample positions of LETR16-5 and LETR16-69 is characteristic for the site and can be linked unambiguously to profile AB (Fig. 5B).

2.4. Micromorphological analysis

Within soil sample LETR16-129 (a monolith tin of 50 × 15 × 10 cm), five overlapping subsamples were taken with Kubiena tins (10 × 7 × 2.5 cm) (Fig. 5A, 5B and 6). The samples were oven-dried and then impregnated with polyester resin. Once the resin was hardened using gamma irradiation, a thin section was sliced from the sample block and attached to a microscope slide. It was ground, polished and lapped to a thickness of about 30 μm and a cover slip was mounted. The resulting thin section slides were scanned on a flatbed scanner and subsequently studied using a Zeiss Axioskop 40 polarization microscope with a mounted MRc5 digital camera.

2.5. Sedimentological analysis

Sample set LETR16-128 consists of 46 samples obtained directly from subprofile BC with a sampling resolution varying between 5 and 1 cm (Fig. 5A, 5B and 6). From each sample, approximately 2 g of sediment was prepared for particle size analysis in accordance with Konert and Vandenberghe (1997). The grain size distributions of the samples were measured using a Sympatec Helos laser particle sizer. Sample LETR16-5 (a monolith tin 50 × 15 × 10 cm) was subsampled continuously per centimetre to analyse sediment grain size and shape (Figs. 5B and 7). The samples (about 2 g) were prepared in accordance with Konert and Vandenberghe (1997). Grain size and shape were determined using dynamic image analysis (Sympatec Qicpic), and grain size-shape distributions were constructed in accordance with the method outlined by Van

Fig. 3. The Leusden-Den Treek study site. A) excavation trench 5, looking northwest. The arrows indicate the Usselo paleosol. B) excavation trench 5 (right) with profile AD, and excavation trench 6 (left), looking southwest. C) excavation trench 5, *Pinus* tree LETR16-54, looking southwest.

Hateren et al. (2020).

A new method – end-member modelling of grain size-shape distributions – was applied to sample LETR16-5 to establish the sediment transport mechanism (Van Hateren et al., 2020) (Fig. 7). Four aeolian end members were defined for the grain size-shape distribution dataset for Leusden: a coarse bedload (EM1); a fine bedload (EM2); a modified saltation load (EM3); and a suspension load (EM4). Proportions of the end members were established for each subsample and used as a proxy for wind strength, vegetation density and surface humidity.

2.6. Analysis of organic content

Samples LETR16-69, LETR-222 and LETR-223 (all monolith tins 50 × 5 × 5 cm) were subsampled continuously every 1.0 cm to determine the organic matter content using Loss on Ignition (LOI) following Heiri et al (2001) (Fig. 5A, 5B, 8, S1a and S1b). The approx. 1 cm^3 subsamples were dried in ceramic crucibles overnight at 105 °C, weighed, and ashed at 550 °C for 4 h, after which they were weighed again. The resulting LOI represents a record of the organic matter content expressed as weight percentage of removed organic matter relative to the dry weight.

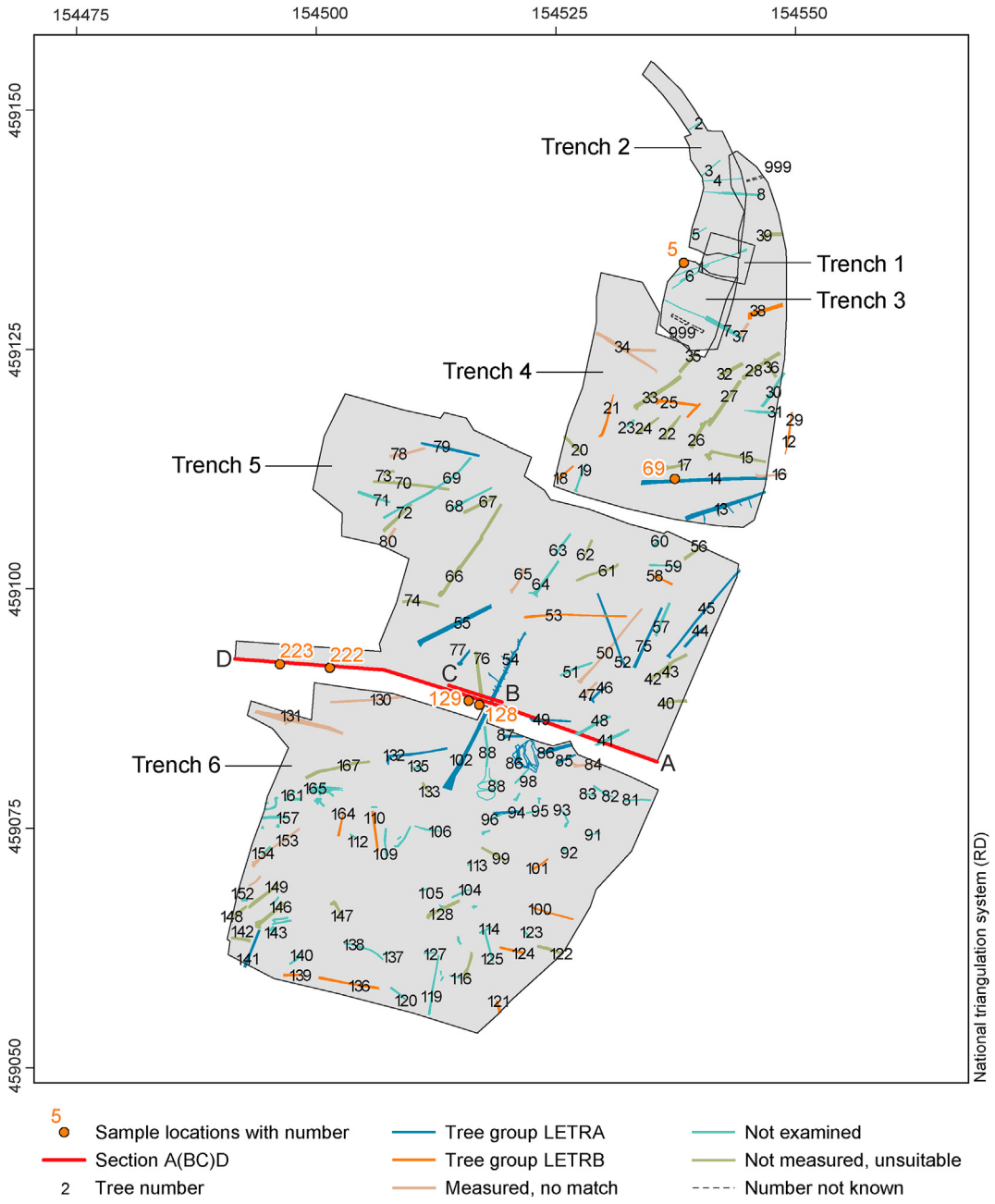

Fig. 4. Excavation plan with the location of all trees and the samples selected for analysis. Excavation trenches 1 to 6 (grey) with section A(BC)D (south side of trench 5) and sample locations (LETR16-5 (trench 3), LETR16-69 (trench 4), LETR16-128, LETR16-129, LETR16-222 and LETR16-223 (trench 5). National Triangulation System (RD) in m. North up.

2.7. Geochemical analysis

After sampling for sedimentological and micromorphological purposes, sample tin LETR16-129 was dried at 40 °C for seven days to enable handheld (HH) XRF analyses (Fig. 5A, 5B and 6). The analyses were carried out using a handheld Thermo Scientific Niton XL3t GOLDD + energy-dispersive XRF analyser equipped with a silicon drift detector. The HH XRF analyser was vertically mounted, pointing downward in a fixed position. The sample tin was moved every centimetre, supported underneath by two lab jacks. The machine built-in Cu/Zn mining mode was used, with a measuring time of 110 s, at four sequential energy settings: light range (Mg to Cl) at 8 kV 200 mA (40s); low range (K to Ti) at 20 kV 100 mA (20 s); main range (V to Ag including L-lines for Pb) (40s); and high range (Cd–Ba), both at 50 kV, 40 mA (10s). Since factory calibrations are a potentially serious source of error when using HH XRF, the machine calibration was checked and adapted using a set of 14 powdered ISE standard samples (Van Dijk and Houba, 2000). Accuracy was tested using the BAMS005B glass standard.

2.8. Palaeoecological analysis

Monolith tins LETR16-69, LETR16-222 and LETR16-223 (50 × 5x5 cm) were subsampled continuously every 1 cm, and in some cases every 0.5 cm (Fig. 5A, 5B and 8 and supporting data Figs. S1a and S1b). Samples were prepared (about 0.7 cm^2 each) for the study of pollen and non-pollen palynomorphs in accordance with Faegri and Iversen (1989). Pollen nomenclature is based on

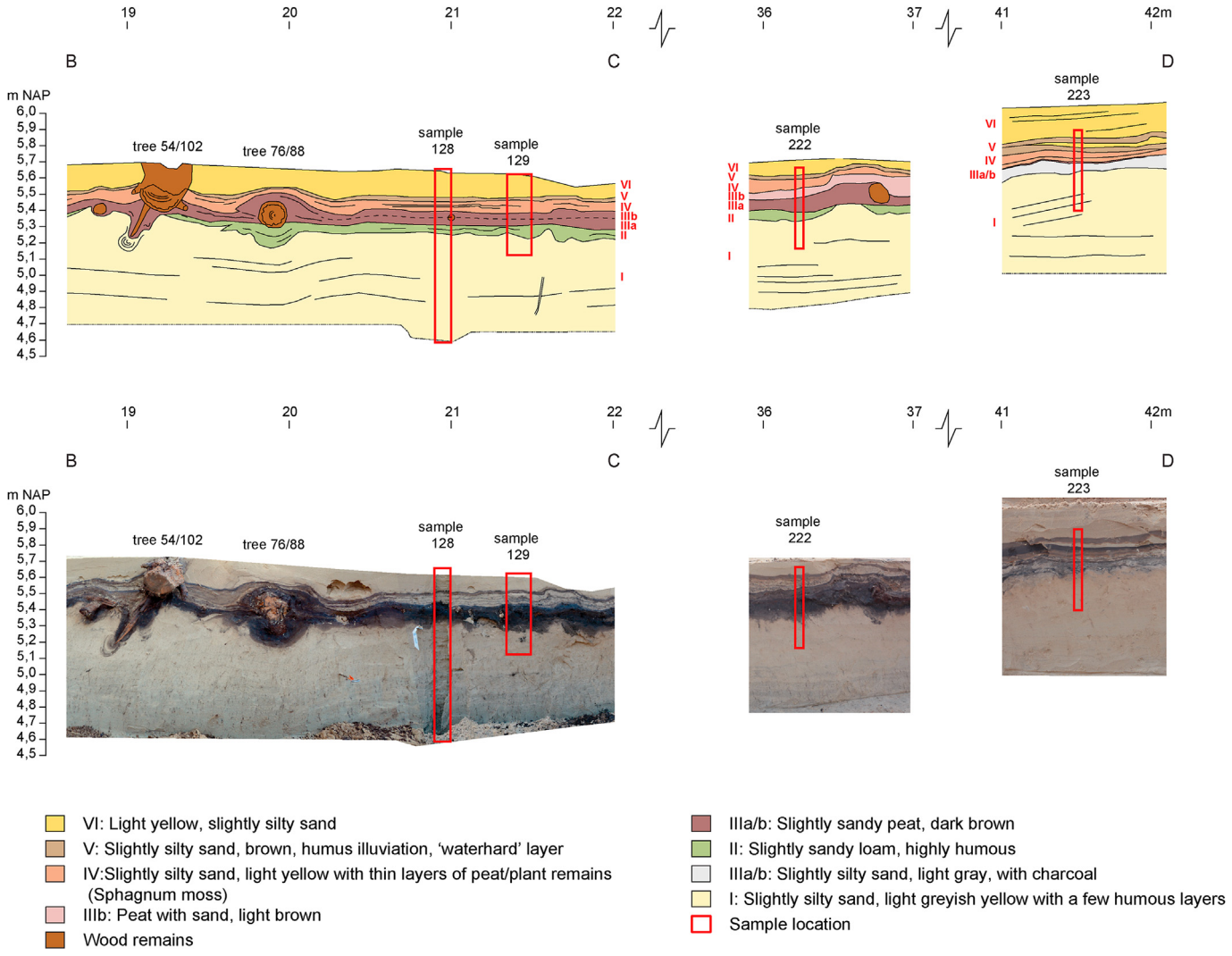

Fig. 5. A. Geological cross-section BD. See Fig. 4 for the location of this cross-section. Bottom: photo composite of the cross section BD of trench 5. Top: lithostratigraphical interpretation (Units I-VI) of the cross section BD of trench 5 with sample locations LETR16-128, LETR16-129, LETR16-222 and LETR16-223. B. Schematic overview of the lithostratigraphical interpretation of cross section BD (left) and the samples LETR16-128, LETR16-129, LETR16-222, LETR16-223 (all trench 5), LETR16-69 (trench 4) and LETR16-5 (trench 3). The stratigraphy at the sample positions of LETR16-5 and LETR16-69 is characteristic for the site and can be linked unambiguously to profile AB. Units used in micromorphological and grain size analysis (1–16) (Fig. 6); paleoecological analysis (AZ1-5) (Fig. 8, Fig. S1 and Fig. S2) and end-member modelling of grain size and grain shape (A–D) (Fig. 7) are indicated. Table 1 presents a concordance of the units used. As a result of cryoturbation, a significant portion of the stratigraphy in LETR16-129 is at an angle of 35°. The legend of Fig. 5A is also applicable to Fig. 5B.

Beug (2004). The remaining sediments in the metal sample box of LETR16-69 were used to study macrofossils (seeds, fruits, vegetative plant remains, bryophytes, Coleoptera (Table S2 for Coleoptera). The macrofossils were prepared in accordance with Mauquoy and Van Geel (2007). Fifteen samples of macrofossils were selected for ^{14}C analysis.

2.9. Dendrochronological analysis

Based on a visual inspection, an estimate was made of the total number of tree rings per sample. Of the 181 wood samples, 52 containing >~40 tree rings were selected for dendrochronological analysis (Figs. 9 and 10). The ring patterns on the cross section were cut with razor blades to enable precise visual identification of the ring boundaries using a Leica M3C microscope. In addition thin sections were used to enhance the identification of segments with very narrow tree rings. Measurements of the annual growth widths were made using a measurement table from SCIEM with an accuracy of 0.01 mm. Measurement series from one or multiple stem disks from a single tree trunk were averaged into one tree series so that each measurement series represented a single tree. Each stem disk was photographed, and for each disk metadata were collected in fact sheets (Fig. S3).

Cross-dating, chronology building and data verification were performed with software programs PAST4 (Knibbe, 2008), PAST5 (Knibbe, 2014) and COFECHA (Holmes, 1999) following standardization of the measurement series in accordance with Hollstein's formula (Hollstein, 1980). Cross-dating measurements were compared using standard dendrochronological cross-dating statistics: Student's t-values based on cross-correlation coefficients (r) between the detrended measurement series (t_{Ho}) and the percentage of parallel variation ($\%PV$) with its significance level (p) (Eckstein and Bauch, 1969).

In order to identify years of reduced tree growth, age trends

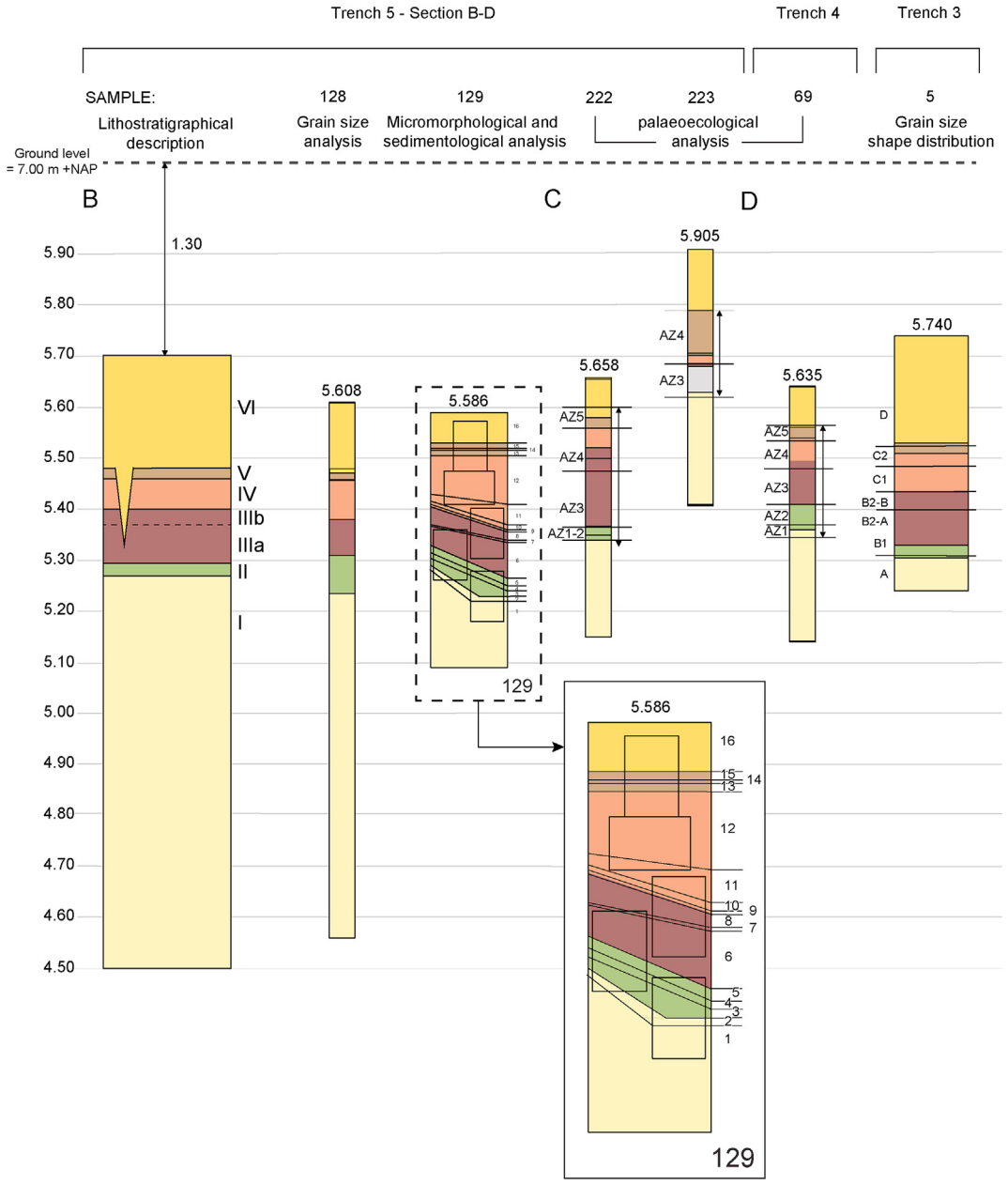

Fig. 5. (*continued*).

were removed by transforming the raw measurement series (TSs) into growth indices using a 128-year spline with 50% variance cut-off (Cook et al., 1990). For each year, the narrowest (x_{min}) and widest growth (x_{max}) index of the underlying index series was determined in order to identify the years in which tree growth in each chronology in all likelihood mirrors the same growth-limiting forcing(s) (Jansma, 2020). These numbers were multiplied ($x{=}x_{min}{*}x_{max}$), which after normalization ($\frac{x-\bar{x}}{\sigma(x)}$) resulted in an annually-resolved stress-based time series. Negative pointer years (PYs) in the wood, defined here as calendar years during which >70–75% of the TSs in each tree group (TG) showed reduced growth relative to the immediately preceding year, were used on identified stress intervals to determine the years of impact more precisely (Schweingruber et al., 1990). The resulting series of negative-impact years (Mi) reflects the overall strength of the environmental impacts on tree growth in each chronology. Intervals of negative impacts lasting ≥3 years were considered to be an indication for severe and prolonged environmental stress (Fig. 11).

2.10. ^{14}C analysis

Initially, fifteen samples of botanical macro-remains from sample LETR16-69 and four samples from one tree (sample LETR16-55 = stem disk LETR00040) were pretreated using standard ABA protocols (Dee et al., 2020). ABA (Acid-Base-Acid) is a standard chemical pretreatment protocol to remove contaminants. The first acid step removes carbonates, the base step removes humic soil substances, and the final acid step removes any atmospheric CO_2 adsorbed during the second step (see Table S4 for all ^{14}C samples). During the pretreatment it was observed that there was an unusual discolouration during the alkalic step. All samples were analysed at the ^{14}C laboratory of Groningen University (Tables S4a and S4b). The results were disregarded because they were all younger than

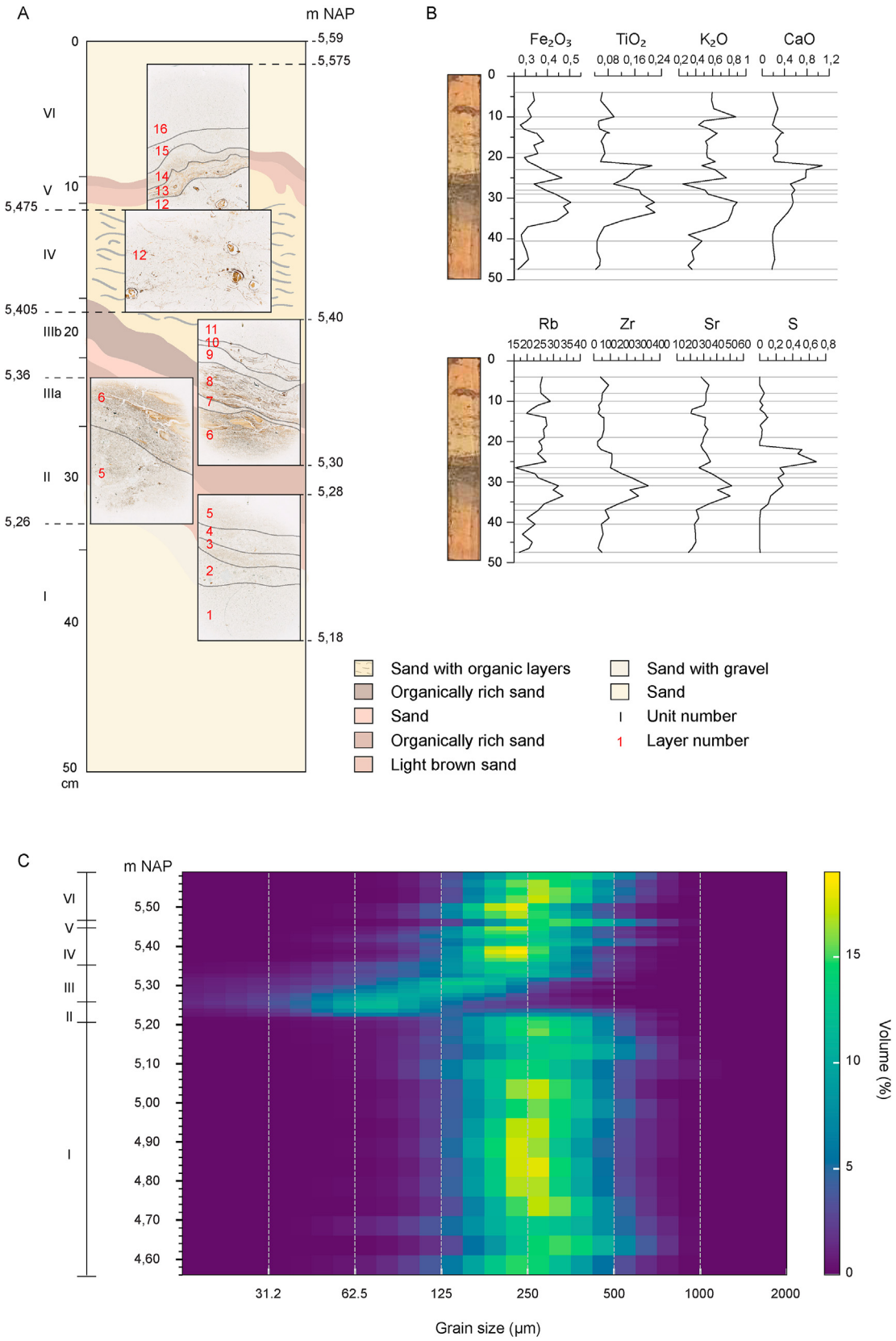

Fig. 6. Micromorphological, HH XRF and grain size analysis. A) five overlapping thin section slides (10 × 7 × 1.5 cm) within LETR16-129 (a monolith tin 50 × 15 × 10 cm) with micromorphological interpretation (unit 1–16). As a result of cryoturbation, a significant portion of the stratigraphy in LETR16-129 is at an angle of 35°. B) Hand Held XFR analysis of LETR16-129. C) grain size analysis of LETR16-128.

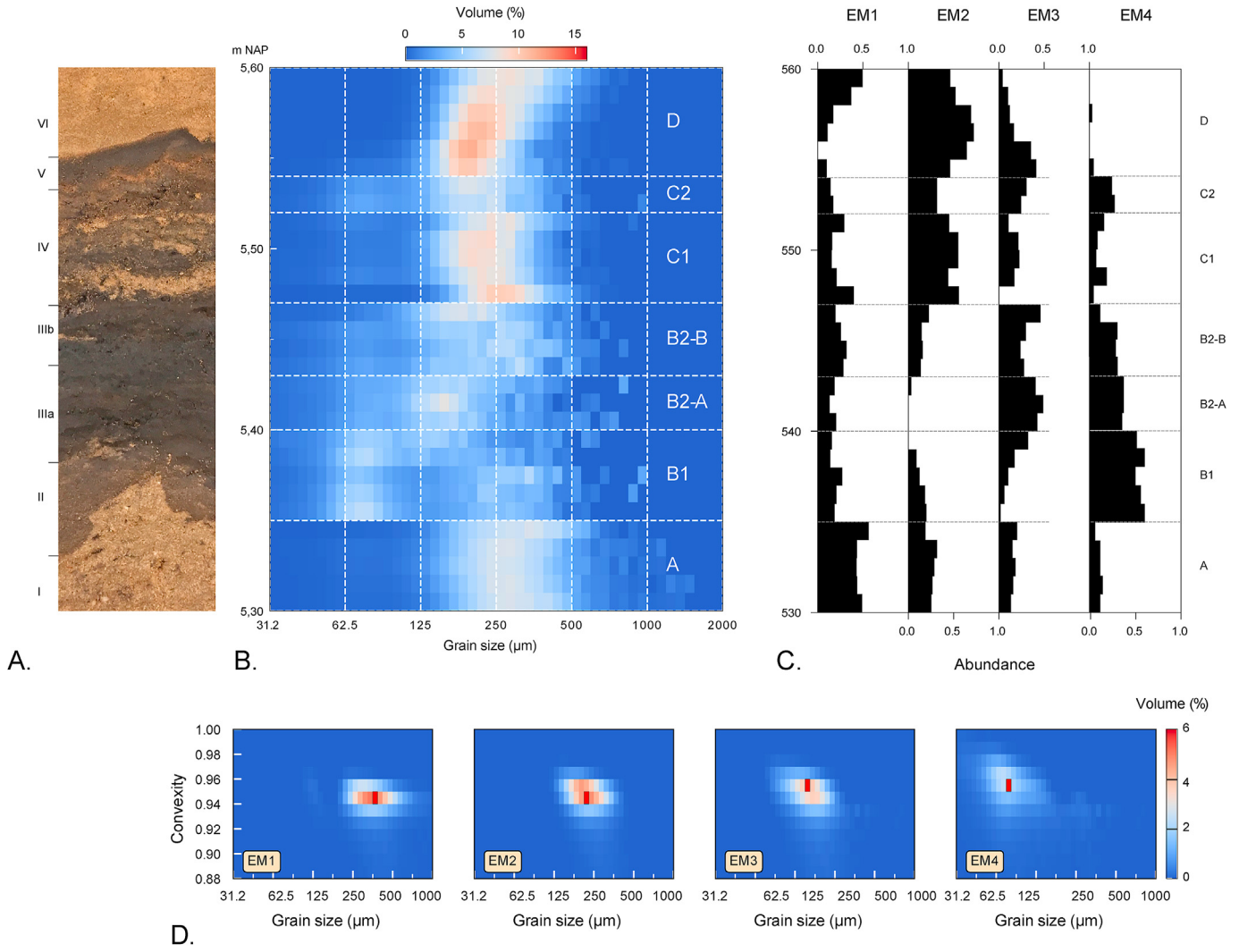

Fig. 7. End-member modelling of sample LETR16-5. A) sampling position. B) grain size analysis. C) end-member modelling, EM1: coarse bedload; EM2: fine bedload; EM3: modified saltation load; and EM4 suspension load (after Van Hateren et al., 2020); D) grain size (in µm) and grain shape (the ratio between convex hull length and perimeter length) distribution of four end members.

expected by the order of several hundreds of years (with one exception of Younger Dryas age). As mentioned above, during fieldwork the presence of a brownish-black humous jelly (dopplerite) was established, indicating potential contamination. An untreated dopplerite sample taken from below a tree remain was subsequently dated to 5480 ± 25 BP (GrM 17567). To deal with this serious issue of contamination it was decided to continue the dating programme with a more intensive pre-treatment including a bleaching step (Tables S4c-S4f). This is suitable for wood samples but not for macro remains. Wood samples were pretreated to alpha cellulose using the method described by Dee et al. (2020). The alpha cellulose was combusted to CO_2 using an elemental analyser connected to a stable isotope mass spectrometer (EA/IRMS, Elementar vario ISOTOPE Cube™/Isoprime 100™). The latter provided the stable isotope ratio $\delta^{13}C$ (in ‰, relative to the VPDB standard; Mook, 2006). Part of the CO_2 was transferred into graphite, by a reaction with H_2 gas at a temperature of about 600 °C, using Fe powder as a catalyst (Aerts-Bijma et al., 2001). The graphite was pressed into target holders for the ion source of the AMS. The AMS is a MICADAS-17 (IonPlus® Mini Carbon Dating System; Synal et al., 2007) manufactured by IonPlus, installed in 2017. The present Groningen laboratory code is GrM. The radiocarbon dates are reported in BP by convention (Van der Plicht and Hogg, 2006), using the oxalic acid reference, the conventional half-life and isotopic fractionation correction with the $\delta^{13}C$ measured by the AMS. The uncertainties of the ^{14}C dates are based on counting statistics and include an estimate for internal laboratory error. The ^{14}C dates are calibrated and/or wiggle-matched to the latest calibration curve IntCal20 (Reimer et al., 2020), using the OxCal software (version 4.4 (Bronk Ramsey, 2009),). The calibrated ^{14}C dates are reported in calBP, i.e. calendar years relative to 1950 CE.

3. Results

3.1. Geological, pedological and palaeo-environmental setting

As mentioned above, a lithostratigraphic description of subprofile BC (Fig. 5A and 5B and Table 1) was made in the field. Six units (I-VI) were distinguished. In addition, micromorphological (LETR16-129) (Fig. 6A), sedimentological (LETR16-5 and LETR16-128/236) (Fig. 6C; Fig. 7B), palaeoecological (LETR16-69, LETR16-222 and LETR16-223) (Fig. 8, S1a and S1b; Table S2) and HH XRF analysis (LETR16-129) (Fig. 6B) were performed. Fig. 5B provides an overview of all samples included in the analysis against the

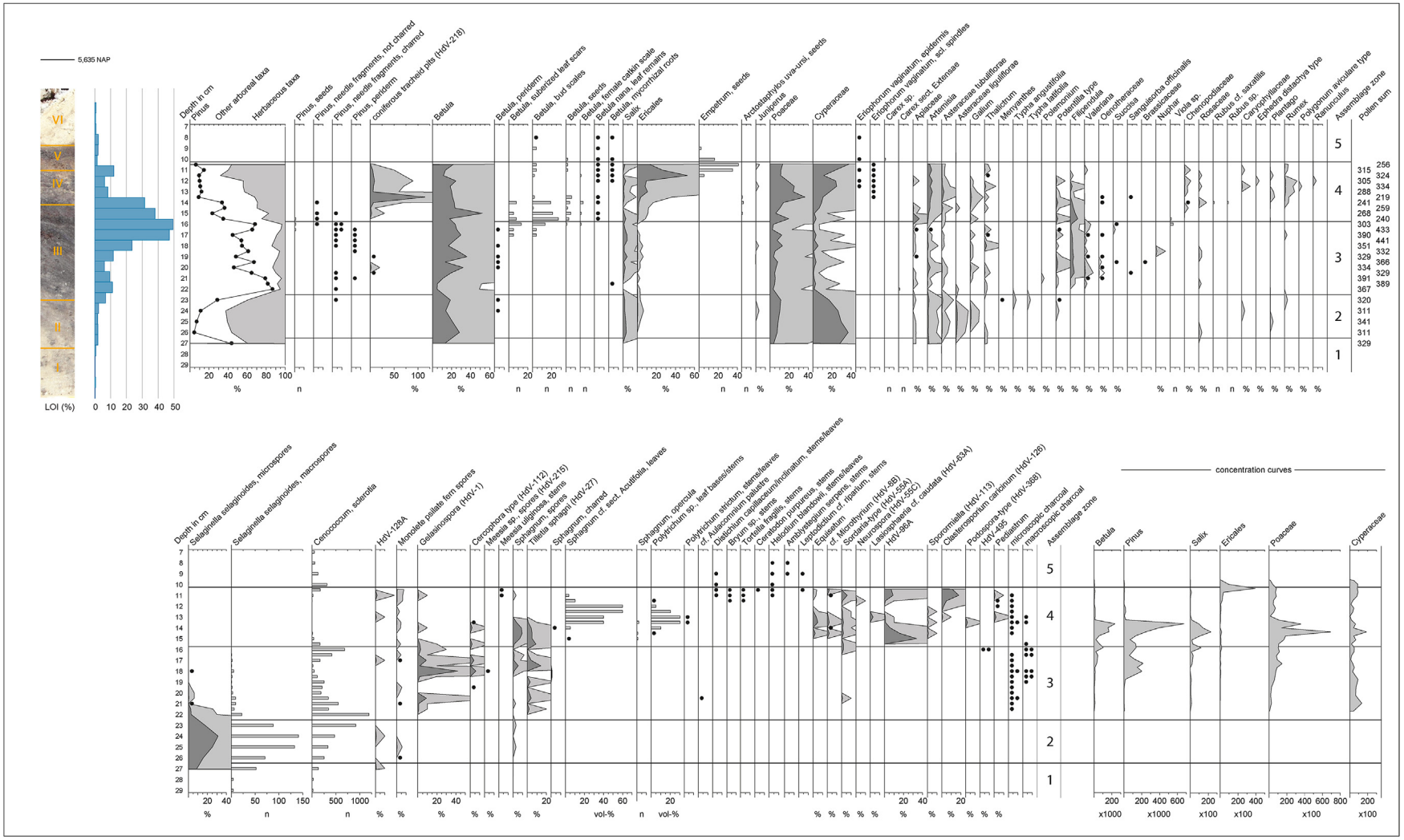

Fig. 8. Palaeoecological analysis. Photo of section LETR16-69 with lithostratigraphycal units I-VI (see Fig. 5A and B), LOI (%) analysis, a combined pollen and macrofossil diagram (seeds, fruits, vegetative plant remains, bryophytes) and pollen zonation (AZ1-5). Pollen data are shown as percentages. Plant macrofossil data are shown as concentrations (histograms) or presence (black dots). See S1A and S1B for LOI analysis, lithography and pollen diagram of LETR-222 and LETR16-223.

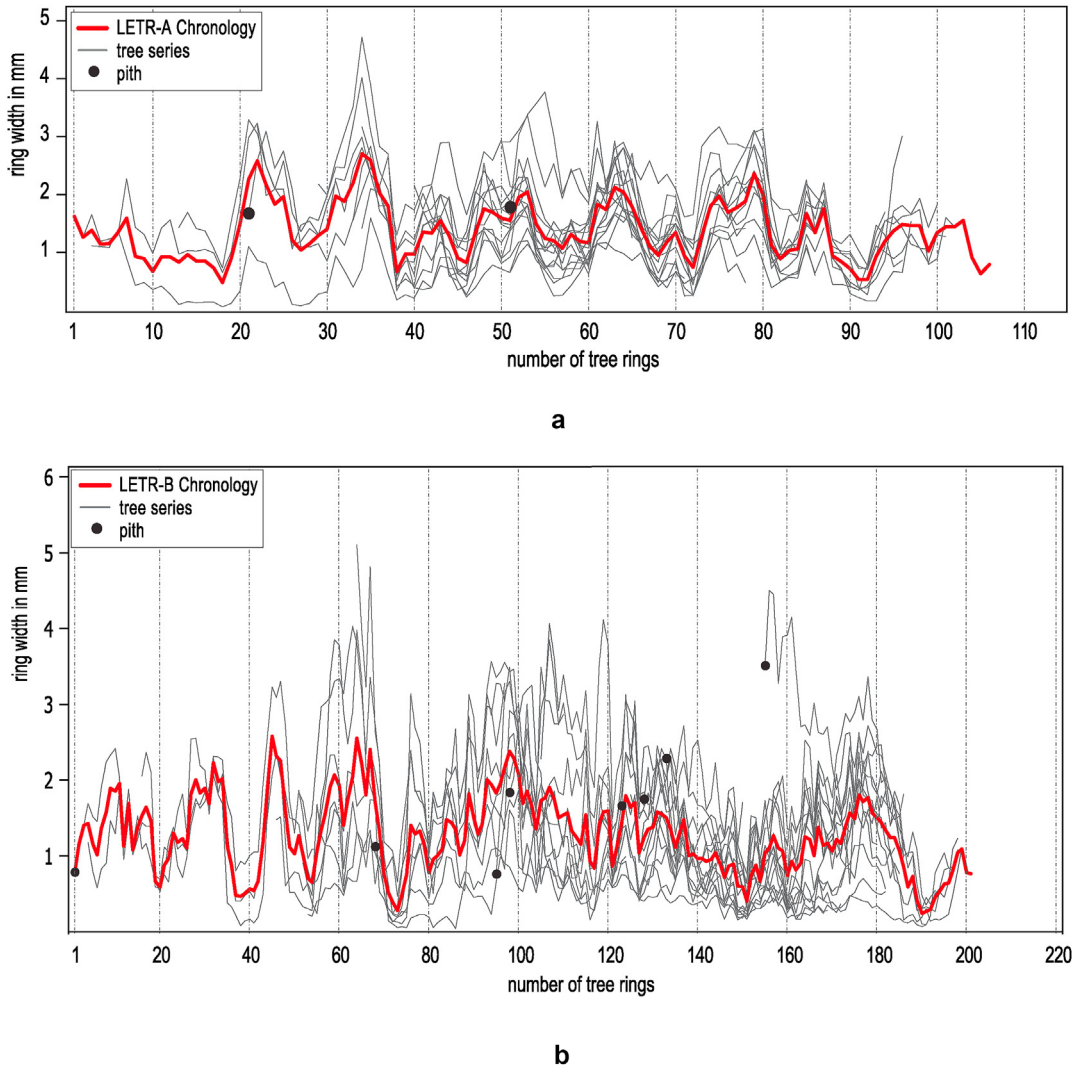

Fig. 9. Dendrochronological analysis. Top: chronology LETR-A (n = 16, 106 years; average value %PV: 76.5; average value t_H: 7.64). Bottom: chronology LETR-B (n = 24, 201 years; average value of %PV: 73.6; average value of t_H: 6.49).

lithostratigraphic background. Table 1 offers a schematic overview and concordance of the units that were distinguished on the basis of lithostratigraphy and grain size analysis (Units I-VI), micromorphology (Unit 1–16), end-member modelling of grain size-shape distribution (Unit A-D), and palaeoecology (AZ1-5). For HH XRF and Coleoptera analyses no additional divisions were made. For the sake of brevity, Table 1 gives an overview of the results of all analyses, excluding the dendrochronological and ^{14}C results.

3.2. The subfossil woodland remains

3.2.1. Observations during fieldwork

During the fieldwork, 165 individual pines and two individual birches were retrieved. As observed in the field, the trees were located in or on top of lithostratigraphic Unit IIIa (Fig. 5A and Table 1). In almost all cases, the trees consisted of trunks without branches or bark, which indicates that they had fallen well after they died. For most specimens, the direction of falling lay between north and northeast. In most instances, the trees had broken off above the stump. However, sometimes the tree trunk took all or part of the stump with it when it fell, or even the entire root system. The trees were superficially rooted and had no taproots. This probably indicates a relatively high water table. Hair roots, however, penetrated deep into lithostratigraphical Unit I. Extensive post-depositional degradation was visually observed in many trunks. In some cases, seen from a cross-section perspective of the tree trunk, only the lower half was preserved. Occasionally, fire damage on the outside of the trees was observed, sometimes only on the upper side of the trunks that was exposed to the air after the tree had toppled over. No macroscopically-visible *Pinus* cone remains were found (see Polak, 1963 for a Dutch site with cones).

3.2.2. Dendrochronological analysis

Dendrochronological analysis of 52 pine samples (*Pinus sylvestris*) resulted in 52 series coded LETR0010 to LETR0520, which represent 49 Tree Series (TSs) since one tree was represented by three samples, and another by two samples (Fig. S3). No bark or waney edge was observed on the 52 stem disks, which eliminates the study of dying-off phases in this woodland. No evidence was found of fire scars, i.e. burnt tree rings that were later overgrown. Based on statistical agreement, visual agreement and COFECHA calculations, sixteen tree-ring series were assigned to the first tree group, resulting in the LETR-A chronology (106 years; average value % PV: 76.5; average value t_H: 7.64) (Fig. 9A). Twenty-four other tree-ring series were

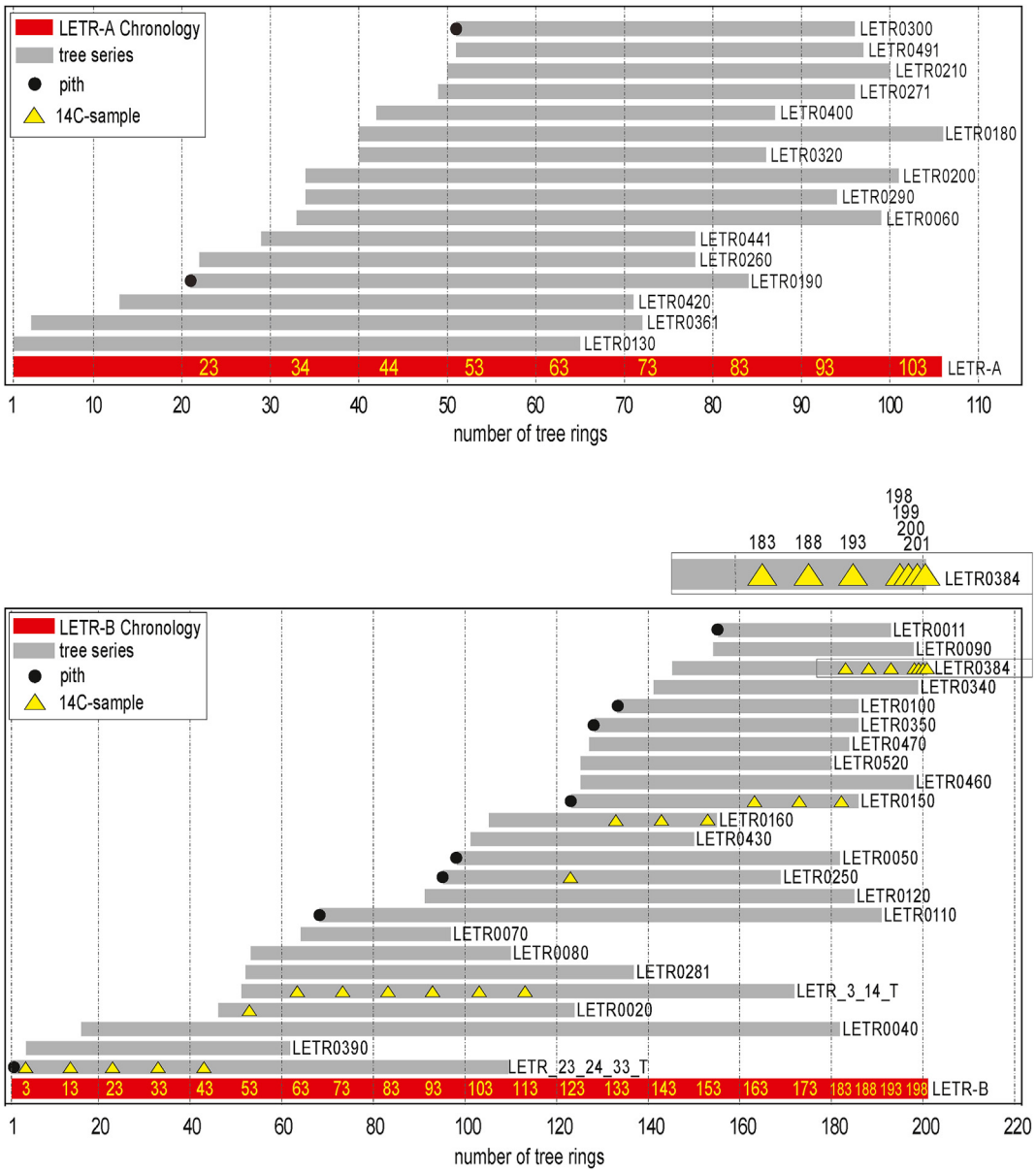

Fig. 10. Tree-ring chronologies and individual tree series with pith shown (dot). Top: chronology LETR-A. Bottom: chronology LETR-B. The position of ^{14}C samples of individual tree rings is indicated (triangle, see SM Ic and Id). The LETR-A chronology belongs to the interval from c. 13,450–13,396 to 13,370–13,316 cal yr BP. The oldest tree ring of LETR-B dates to between 12,952 and 12,937 and the youngest ring dates to between 12,754 and 12,739 cal yr BP.

grouped together in the second LETR-B chronology (201 years; average value of %PV: 73.6; average value of t_H: 6.49) (Fig. 9B). Nine tree-ring series remain ungrouped, showing little agreement among themselves and with LETR-A and LETR-B (see Fig. S3, for the tree grouping).

As European Late-Glacial tree-ring chronologies are supposed to show strong teleconnection between remote sites (Kaiser et al., 2012), chronologies LETR-A and LETR-B were compared to the Bølling-Allerød dendrochronological chronologies of Warendorf (Warendorf 1), Reichwalde (RW15), the German Danube (LG1_Don7) and Breitenthal (BRE_LG3 and BRE_LG3B) (Kaiser et al., 2012). This did not yield a match, meaning that the Leusden chronologies could not be dated on a calendar time scale using dendrochronology.

Based on observed pith and pith off-set calculations, LETR-A chronology (n = 16) sprouted within a timeframe of about 50 years (Fig. 10A). The chronology has an average ring width of 1.47 (min. 0.09 – max. 4.75 mm) and contains six marked growth reductions lasting from three to five years (Fig. 11A). However, LETR-A shows a more homogenous and healthy increment pattern than LETR-B (see below).

Based on observed pith and pith off-set calculations, new trees from the LETR-B chronology (n = 24) sprouted during an interval of over 150 years (Fig. 10B). The chronology has an average ring width of 1.30 mm (min. 0.01 – max. 5.07 mm) and is characterized by eight significant growth reductions (Fig. 11B). Two are of remarkably long duration: one begins at tree ring 35 (replication n = 3) and lasts for seven years; the other begins at ring 45 (n = 3) and lasts nine years. Although shorter (six years), the growth reduction that begins at tree ring 68 (n = 8) is exceptionally deep. At the end of the series, three consecutive growth reductions are visible (n = 11, n = 3 to 10, and n = 3 respectively). Furthermore, a strong

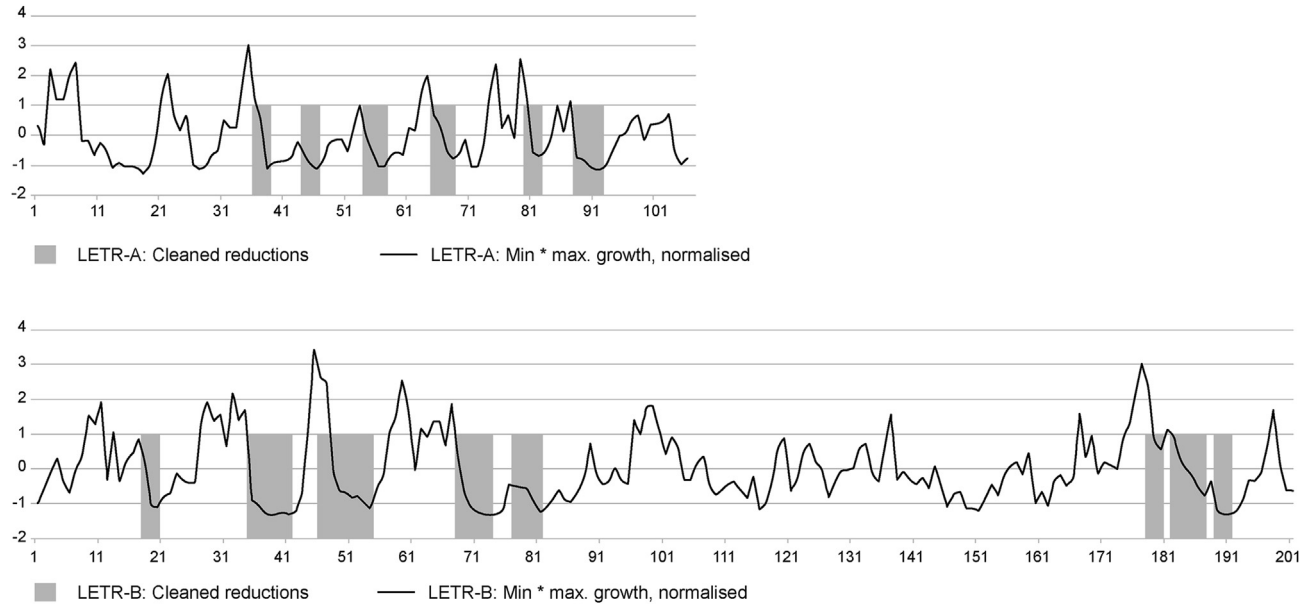

Fig. 11. Environmental impacts on tree growth. Y axis: arbitrary unit for tree growth, for calculation, see Section 2.9. A) Chronology LETR-A (top). B) Chronology LETR-B (bottom). Growth reductions lasting three years or more are indicated in grey.

decrease in annual ring width is detected in the second half of the data, with increments down to 0.04 mm. Given their increased ring width, various tree series testify to better growth conditions between tree rings 165 to 185.

The LETR-A and LETR-B chronologies do not cross-date, indicating that these tree groups grew during different time intervals.

3.2.3. ^{14}C-datings of tree-ring series LETR-A and LETR-B

In total, nine samples from LETR-A (Table S4c), 27 samples from LETR-B (Table S4d), and six from two *Betula* sp trees were subjected to ^{14}C analysis (Table S4e). In addition, nine samples from the outermost ring of *Pinus* trees unrelated to LETR-A or LETR-B were dated using ^{14}C in order to check whether the dataset contains trees that grew here at times not covered by the series contained in LETR-A and LETR-B (Table S4f). The radiocarbon results support the dendrochronological finding that the LETR-A (c. 11,540–11,360 BP) and LETR-B (c. 11,025–10,800 BP) chronologies represent two separate populations. The excavation supports the relative dating of both chronologies, since two trees from LETR-A were uncovered beneath two trees from LETR-B.

The ^{14}C datings for both series were calibrated and wiggle-matched using IntCal20 (Reinig et al., 2020). The LETR-A chronology belongs to the interval from 13,450–13,396 to 13,370–13,316 cal yr BP (all ^{14}C dates are situated on a plateau). The oldest tree ring of LETR-B dates to between 12,952 and 12,937 and the youngest ring dates to between 12,754 and 12,739 cal yr BP (Fig. S5). Although a relatively large maximum counting error occurs in the INTIMATE Event Stratigraphy, it seems plausible to position the death of the LETR-A woodland in the transition from GI-1c to GI-1b (13,311 b2k, max. counting error: 149) and the death of the LETR-B woodland in the transition from GI-1a to GS-1 (12,807 ± 12 calBP) (Reinig et al., 2021). It should be noted that the youngest tree rings of LETR-B fall within the beginning of the steep rise in ^{14}C in earth's atmosphere, which probably resulted from a drop in deep-water formation in the North Atlantic (decline in ocean ventilation) associated with a shift of the Southern Hemisphere westerly winds and increased wind-driven upwelling in the Southern Ocean (Anderson et al., 2009; Toggweiler, 2009; Denton et al., 2010). It is noteworthy that all pines that show no correlation with either chronology belong to the period covered by LETR-B. In all probability, both birch trees are younger than the last pine woodland generation and date to the beginning of the Younger Dryas period.

4. Discussion of site development

The geological, pedological and palaeoecological development of the site can be assessed in detail using the results from the multiproxy analyses. The description below should be read in close connection with (a) the site's lithostratigraphy (Units I-VI) as shown in Fig. 5B and described in Table 1, (b) the underlying data as shown in Fig. 6 (micromorphology, grain size and HH XRF), Fig. 7 (end-member modelling of grain size-shape) and Fig. 8, S1a and S1b (palaeoecology), and (c) Table 1 for the interpretation of these data.

4.1. Unit I (<ca 5.27 m + NAP)

Unit I is approx. 75 cm thick and consists of aeolian sediments. The large proportion of bedload in the upper 10 cm of Unit I indicates an open vegetation cover. This cover comprised dry, pioneer taxa such as *Artemisia*. Quartz is the main mineral deposited during this phase and no indications for transport of silt (zircon) or clay minerals are found (Rb, K_2O). A thin gravel bed several centimetres below the top of Unit I probably indicates sediment winnowing by wind. The *Pinus* pollen present in this unit is probably the product of long-distance transport.

4.2. Unit II (ca 5.27–5.30 m + NAP)

As Unit II shows a dominance of suspension load, the palaeosurface associated with this unit must have been significantly wetter and/or more vegetated to create the quiescent conditions necessary for the deposition of aeolian dust. The increase in zircon and clay mineral indicators towards the top of Unit II is consistent with this finding. Iron content, indicating the transport and precipitation of iron hydroxides, was deposited in the context of later soil formation (see below). Humus and fine, elongated organic material in the top of Unit II may have come from the unit above as

Table 1

Leusden-Den Treek. Lithostratigraphy (Units I-VI) and overview of the results of (1) micromorphological, grain size and HH XRF analysis (units 1–16); (2) End-member modelling of grain size and grain shape (units A-D); and (3) palaeoecological analysis (assemblage zone (AZ) 1–5). The table presents a concordance of the units used.

	Lithostratigraphic description and grain size analysis and LOI										
Sample	Field observation next to LETR16-128 and LETR16-128/236										LETR16-223
Figure(s)	5a, 5b, 6c, 7b										S1
Comments	This desciption fits LETR16-5, LETR16-69, LETR16-128, LETR16-129 and LETR16-222										
m +AOL	Unit	Colour	Laye-ring	Grain size range	Sor-ting	Coarse-ning trend	Illuvia-tion	LOI	Organic material		
7.00		Plough zone									
6.70	VI	Light yellow	++	125-550	high	↑	-	~0	-	Present	
5.48	V	Dark brown	++	50-400	low		++ 'water-hard'	~2-5	-	Present	
5.46	IV	Light yellow	++	100-350	high		?	~2-8	Thin, well-preserved bands of mosses, leaves and twigs, well preserved, poorly humidified	Millimeters thick layer of peat	
5.40	IIIb	Dark brown	++	150-350	low	↑	?	~20-50	Leaves, twigs and mosses, humidified	Light to dark grey, mineral poor, 'leached' sand containing large quantities of charcoal, i.e. classic Usselo soil	
	IIIa	Dark brown	+/- shallow frost cracks in top	80-250	low		?	~5-10	(Root) wood, humidified organic material. Trees in or on top of this unit		
5.30	II	Yellow grey	--	45-100 and 200-400	low	↓	?	~2-6	No (root) wood	Not present	
5.27	I	Light greyish yellow	++	100-500 A very thin gravel bed at ca 5.25 m +NAP (6 7 mm in size).	high		-	~0	Vertical hair roots	Present	

Micromorfological en HH XRF analysis												
LETR16-129												
6a, 6b												
As a result of cryoturbation, a significant portion of the stratigraphy is at an angle of 35o												
Unit	Illu-viation	Laye-ring	Micro-faunal activity	Sand and organic material	Organic content	Char-coal	Quartz 100-all other	Clay Rb, Al_2O_3, Sr	Silt Zr	Iron-ox Fe_2O_3	CaO	
16	-	++	-	Fine	None	-						
15	++	+	-	Fine	Small and amorphous	-						
14			-									
13	-	++	-	Layered organic material interspersed with fine sand	*Betula n.* leaves, twigs, seeds and moss. Fruiting bodies of fungi	-	++	--	--	-	-	
12	-	++	-	Fine to coarse sand with organic material	*Betula n.* leaves, twigs, seeds and moss. Fungi	-						
11	+	++	-	Fine sand layers interspersed with organic material	*Betula n.* leaves and twigs	-						
10												
9											++	
8	-	-	-	Fine and coarse sand with organic material	*Betula n.* leaves, twigs and *Bryophyta* surrounded by fungal spores	-	--	-	-	-	+	
7	+	-	-	Fine sand with organic material	Amorphous	-	--	+	+/-	+	-	
6	+	+	++	Fine sand with organic material	Leaves, pine wood, tree bark and fine organic material, charcoal, phytoliths, mite faeces, fungi	++ unlayered	-	-	++	+	-	
5	-	+/-		Silt and sand with fine organic material	Amorphous	-	-	-	++	++	-	
4	-	-		Fine and coarse sand with fine organic material	Amorphous	-						
3	-	-		Silt and sand with fine organic material	Amorphous	-						
2	-	+	-	Coarse, sometimes extremely coarse sand, few fragments of gravel (6-7 mm)	none	-	++	-	-	+/-	-	
1	-	+	-	Coarse sand	None	-						

End member modelling of grain size-shape distribution				
LETR16-5				
7				
Aeolian				
Unit	EM1 coarse bedlo	EM2 fine bedload	EM3 modified saltatio	EM4 sus-pension load
D				nil
C2				
C1		high ↑	low ↓	low ↓
B2B	↑	low	↓	↓
B2A	low	nil	high	↓ high
B1	low	low	↑ low	high
A	high	high	low	low

EM unit	Palaeoecological analysis																
	LETR16-69, LETR16-222, LETR16-223																
	8a, S1																
	Pollen	*Pinus* pollen	*Pinus* macro	*Betula spp.* pollen	*Betula spp.* macro	*Betula nana* macro	*Salix*	*Ericales*	*Empe-trum*	Upland herbs	Marsh herbs	*Filipen-dula*	*Sphag-num*	*Bryo-phythes*	*Selaginella sel.*	*Cenococ-cum* scletoria	*Gelasino-spora*
D, C2	poor			↓				↑	↑	↓	↓						
C1, B2B	good	low ↓↓	+ tracheid pits	++	++	++ ↑↑	+ ↓	++ ↑↑	↑	++	++		↓↓ domi-nant ↑↑	++ (non Polythri-chum) *Polythri-chum* ↑↑			
B2A	good	high	+ epidermis fragm. of needles; periderm	high	+		+			+	+		spores and *Sphagnum* parasite			++	++
B1	good	↑ low		+			+			+	+				dominant (micro- and macrspores)	++ ↑	
A	poor	high													macro-spores		

a result of bioturbation. Pollen analysis indicates a pioneer vegetation of *Selaginella* (microspores and macrospores) with *Betula* (both *B. pubescens/pendula* trees and *B. nana* shrubs), *Salix*, Poaceae, Cyperaceae, *Artemisia,* other Asteraceae, *Galium* and *Thalictrum* (biostratigraphic zone 2a1 *sensu* Hoek (1997); Fig. 1). The proportion of suspension declines gradually through loamy Unit II, whereas the proportion of modified saltation increases. This may indicate a desiccation of the paleosurface. In the top of unit II and in the overlying unit the remains of the oligophagous *Pinus* infesting bark beetle *Thomicus minor* and the root-feeding *Othiorhynchus ovatus* are found, indicating the local presence of *Pinus.*

4.3. Unit IIIa (ca 5.35–5.30 m + NAP)

Unit IIIa shows a (further) decrease in suspension load and a (further) increase in modified saltation. This was caused by an increase in woodland coverage. The geochemical mineralogical signal is diluted by the increase in organic matter, indicating decreasing mineral input. In fact, the litter layer or A-horizon (micromorphological unit 6), which contains loose and unlayered fragments of charcoal, phytoliths, leaves and mite faeces, is preserved at the site. Bioturbation is visible in Unit IIIa as microfauna and fungi actively decomposed the organic matter. Eluviation of humus from Unit IIIa produced illuviation in the underlying Unit II. The latter is also indicated by an increase in iron and clay indicator elements in Unit II (see above).

The pollen samples reflect a local, open *Pinus-Betula* woodland at the sampling site, with high pine pollen percentages, epidermis fragments of pine needles and *Pinus* periderm (biostratigraphic zones 2a2 and 2b *sensu* Hoek (1997); Fig. 1). The pollen percentages of several taxa are relatively low because of the extremely high frequency (overrepresentation) of locally produced pine pollen grains. The organic content of the macrofossil samples shows a strong increase, which roots will have contributed to. The pollen curves of *Salix*, Poaceae, Cyperaceae and *Artemisia* suggest that there was no closed forest here. Furthermore, *Filipendula* (meadowsweet) grew in moist open places in the pine-birch woodland. Spores of the fungus *Gelasinospora* show that dry phases and fires occurred intermittently. Macrofossils of *Sphagnum* were not preserved, but the occurrence of *Sphagnum* spores and the presence of spores of the *Sphagnum* parasite *Tilletia sphagni* point to the local occurrence of *Sphagnum*. The presence of the beetle *Cyphon* sp. indicates the nearby presence of surface water. The *Pinus* infesting bark beetle *Thomicus minor* is accompanied by *Glischrochilus quadripunctatus* frequenting burrows of *Thomicus*.

Pollen analysis of Unit IIIa shows two distinct *Pinus* pollen maxima which can most probably be linked to two successive woodland phases. The first arrival of *Pinus*, represented by chronology LETR-A, is securely dated at 13,425 ± 25 cal yr BP. Taking into account the pith off-set and possible missing outer rings, this series represents more than 120 years of woodland growth. A second generation of woodland growth is securely dated at c. 12,952–12,937 cal yr BP and is represented by chronology LETR-B. Taking into account the pith off-set and possible missing outer rings, LETR-B represents over 220 years of woodland growth. A comparison of the average ring width of LETR-A and LETR-B indicates relatively less favourable local growth conditions during the time interval covered by LETR-B than during its predecessor LETR-A (see above). The distribution of pith dates during both forest phases points at that trees from both series did not sprout at the same time, indicating prolonged intervals of relatively favourable germination conditions.

On a regional scale, the establishment of a pine woodland must have stabilized the landscape, thereby impeding aeolian bedload transport and reducing the size of dust-generating sand-seas. The source of the suspended load (dust) will have been confined to distant sources. On a local scale, the year-round evapotranspiration of *Pinus* may have caused drier surface conditions, especially on the topographic highs surrounding the depression in which the subfossil pine woodland was found. Conditions on these neighbouring highs may have been dry enough for localized remobilization of the coversand. Sediment would then have been carried from the hights into the depression in modified saltation (i.e. very short-term suspension).

4.4. Unit IIIb (ca 5.0–5.35 m + NAP)

The top of Unit IIIa and bottom of Unit IIIb show a minor decline in surface stability marked by an increase in the amount of coarse and fine bedload. This is also indicated by an increase in quartz and Zr, which shows an increase in fine sand/silt. This unit is again completely quartz dominated. However, modified saltation and suspension remain dominant because of the presence of a herbaceous vegetation and humid surface conditions. The transition from Unit IIIa to IIIb – immediately after the highest LOI value – corresponds to the changeover from pollen zone 2b to 3a (start of the cold Younger Dryas) as defined by Van Geel et al. (1989) and Hoek (1997), characterized by a sharp decline in *Pinus*, an increase in *Betula* and an increase in herbaceous taxa (*Artemisia*, Chenopodiaceae, Cyperaceae, Ericales, Poaceae, *Rumex*). *Betula* sp. including *B. nana*, expanded considerably during this phase, after the dying-off of *Pinus* trees and the appearance of open space in the (former) pine woodlands. A decline in *Pinus* pollen coincided with finds of *Pinus* tracheid pits. The presence of these small wood particles points to highly decomposed, disintegrating pine wood. As at Usselo (Van Geel et al., 1989), a temporary, dense *Sphagnum* vegetation developed at the damp, acidic, oligotrophic sample site, containing *Polytrichum strictum* and *Eriophorum vaginatum*. An increase in Ericales pollen halfway Unit IIIb is linked to the presence of *Arctostaphylos uva-ursi* and later of *Empetrum*. Other taxa in the regional vegetation were Poaceae, Cyperaceae, *Rumex*, Chenopodiaceae and *Artemisia*. Coprophilous fungi (*Sordaria* type, *Sporormiella*, *Podospora* type) indicate the presence of herbivorous mammals in the landscape. Where the *Sphagnum* phase shows a decline, some other bryophytes appear: *Bryum* sp., *Distichium capillaceum/inclinatum, Tortella fragilis, Ceratodon purpureus, Helodium blandowii, Amblystegium serpens and Leptodictium* cf. *riparium.* The appearance of these bryophytes reflects the transition from the acidic *Sphagnum* phase, when soils in the region were acidic and still covered with vegetation, to a dynamic phase of cold climate, open soils, erosion and the deposition of lime-rich coversand at the sampling site. There was no longer soil activity by microfauna, but organic material was actively decomposed by fungi. The Coleoptera provide a clear indication of climate change at the transition from IIIa to IIIb, with the replacement of species now present in the Netherlands by species of northern or alpine zones where conifers are sparse or not present (*Eucnecosum brunescens*, *Diacheila arctica* and *Agonum consimile*).

4.5. Unit IV (ca 5.46–5.40 m + NAP)

The base of aeolian Unit IV reflects the continuation of a cold climate and lower temperatures. The landscape must have opened up significantly as fine bedload dominates the sediment deposition. This unit is quartz dominated as is shown by a relative increase of SiO_2 over finer clay (Rb and K_2O) and silt (Zr). This indicates an increase in wind speed as the transport of coarse, quartz rich material is dominant and fine material becomes diluted or is not deposited at the site or transported further away. Transport and sedimentation of coarse grain size quartz will have led to a high

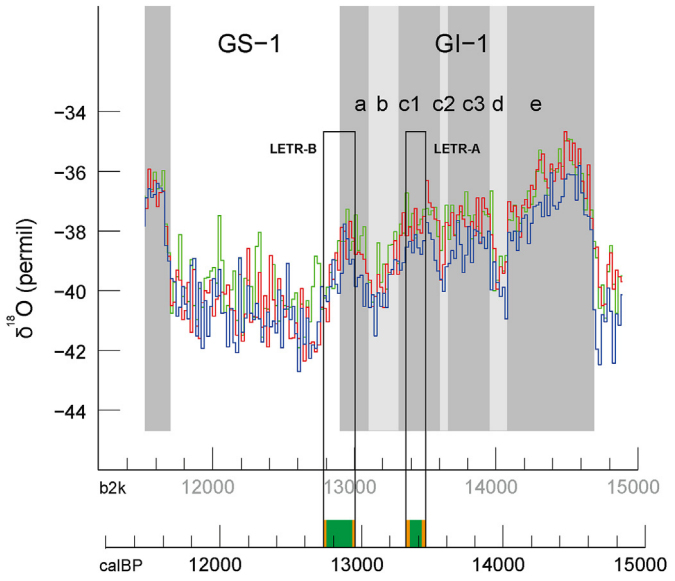

Fig. 12. Comparison of the wiggle matched ^{14}C dates of Leusden-Den Treek chronologies LETR-A and LETR-B (calBP) and the 20-year average value of $\delta^{18}O$ (VSMOV) for GS-1 and GI-1 from the Greenland ice-core records GRIP (red), GISP2 (green) and NGRIP (blue) on the GICC05modelext time scale (b2k) (adapted from Rasmussen et al., 2014). The INTIMATE event stratigraphy is shown with interstadials illustrated by grey shading (light grey indicating cold sub-events). Note that the maximum counting error for the start of GS-1 (at 12,896 b2k ± 4) in the INTIMATE event stratigraphy is 138. According to Reinig et al. (2021), however, new evidence shows that the well-dated isotopic Al/YD transition in annually resolved European varved records is synchronous with the climate transition in Greenland from GI-1 to GS-1. (For interpretation of the references to colour in this figure legend, the reader is referred to the Web version of this article.)

local sedimentation rate. The absence of silt and clay minerals also indicates a more open environment. However, a small proportion of modified saltation and suspension sediment remains. These finer sediments may have been deposited during the quiescent conditions of the *Betula nana* growing season. This is confirmed by the pollen spectra featuring not only a wide variety of herbs, with the characteristic taxa *Artemisia* (a pioneer, growing in open areas), Cyperaceae and Ericales, but also *Betula* (largely *Betula nana*) in particular. Sub-arctic species of Coleoptera are a clear indication of a cold climate.

4.6. Unit V (ca 5.48–5.46 +NAP)

Unit V shows a decline in *Betula*, Poaceae and Cyperaceae pollen. *Empetrum* expanded, probably because of its ability to withstand the increase in aeolian activity and cooling climatic conditions. The unit corresponds to biostratigraphic pollen zone 3b (second part of the Younger Dryas) as defined by Hoek (1997). Suspended material is also present in Unit V. As observed in the field, frost cracks penetrated in Unit IV and Unit III, an indication of deeper seasonal frost. In the Holocene, humus illuviation (iron pan or 'waterhard', see paragraph 2.1) occurred at the lithological transition from Unit V to VI. This is also indicated by the increase in elements associated with clay minerals at the base of Section V.

Periglacial conditions during the first and colder half of the Younger Dryas caused cryoturbation of the top of Unit I and Units II-V (Renssen and Isarin, 2001; Hoek and Bohncke, 2001).

4.7. Unit VI (ca 6.70–5.48 m + NAP)

The near-absence of the suspension component in aeolian Unit VI probably indicates very dry conditions and an open Younger Dryas landscape with limited or no vegetation. No indications for deposition of clay minerals or silt are found in this unit as the mineralogy solely consists of quartz.

5. Discussion of the tree-ring data

On the basis of numerous palynological studies of Dutch sites (Van Geel et al., 1989; Hoek, 1997, 2001), Late-Glacial vegetation development in general and Late-Glacial woodland development in particular are well documented. However, the subfossil *Pinus* trees from Leusden provide a more complete picture of Late-Glacial pine woodland stands in the Netherlands. The Leusden pollen and tree-ring data show the occurrence of two successive and temporary phases of pine woodland development. These phases are the result of an interplay between climatological and environmental changes, including hydrological ones. The growth conditions of modern *Pinus sylvestris* can be used to assess these relationships in more detail (see Burns and Honkala, 1990; Nikolov and Helmisaari, 1992).

Pinus sylvestris is adapted to a wide variety of climates as indicated by its extremely wide geographical range. Mature Scots pine has a pronounced drought tolerance and is therefore very undemanding as to water supply. At the seedling stage, however, it has high drought sensitivity (Dulamsuren et al., 2013). *Pinus sylvestris* can grow on the poorest sandy soils, even colonizing acid highland moors (Houstan Durrant et al., 2016) and ombrotrophic bogs (Van Geel et al., 2020). In general, the species has a good frost resistance. It can withstand mean January and February temperatures of below −20 °C (Prentice and Helmisaari, 1991) and winter temperatures of well below −30 °C (Nikolov and Helmisaari, 1992). Near its cold ecotone limits, however, the presence and growth of *Pinus* is dependent on a combination of factors: (1) July and August temperatures, which preferably must be over +8 °C (Grace et al., 1989; Tuovinen, 2005; Konovalov et al., 2019); (2) the length of the growing season, which needs to be more than 105–110 days; (3) an effective temperature sum of over 500 growing degree days (threshold value +5 °C) (Schibalski et al., 2014) or even over 600 (Tuovinen, 2005); (4) an active soil layer temperature of over +5 °C at a depth of 15–20 cm during the growing season (Arzac et al., 2019; Lindholm, 1996); (5) the absence of frozen or very cold soil water in late winter or early spring to avoid foliage death (Grace et al., 1989; Grace and Norton, 1990; Tuovinen, 2005); (6) the absence of snow cover during the start of the growing season; and (7) the presence of rain or melt water in May (Kirchhefer, 2000; Tchebakova et al., 2009). In addition, the ripening limit for *Pinus* seeds is a minimum of +10.5 °C (Lindholm, 1996). The effect of low precipitation on the northern and altitudinal limits of *Pinus* is controversial (Lindholm, 1996 versus Birks and Birks, 2014).

The dating of the older *Pinus* series (LETR-A chronology) is important because until now only one date for *Pinus* charcoal from biozone 2a2 *sensu* Hoek (1997) is known in the Netherlands (Budel) (Hoek, 1997). At Milheeze the presence of *Pinus* is securely dated at the transition from biozone 2a1 to 2a2 (Bos et al., 2006). Although Dutch pollen diagrams show a first slight increase in *Pinus* pollen at the transition from zone 2a1 to 2a2 at around 13,500 cal yr BP (11,500 BP), it is generally assumed that the low relative proportion (<20%) does not indicate migration along a closed front but is more in keeping with an ecotone concept, whereby patches of trees expand in time at favourable sites (Hoek 1997, 2001), such as the leeward side of the ice-pushed ridge of the *Utrechtse Heuvelrug*. The development and death of *Pinus* at Leusden is probably a direct proxy for climate change (Fig. 12). LETR-A (106 years) shows consistent, rather stable annual growth increments, indicating favourable and stable growing conditions. The difference between the average ring width of the series contained in older LETR-A (1.39 mm) and in younger LETR-B (1.24 mm) may indicate higher

annual temperatures or relatively more favourable local growth conditions during the interval covered by LETR-A than by its successor LETR-B. This is consistent with the growth reductions in LETR-B, which are markedly more prolonged than those is LETR-A. It remains possible, however, that local growth conditions were impacted by increased humidity that was less favourable for LETR-B than for LETR-A: pollen analysis shows a marked increase in wetland herb pollen in the upper part of Unit IIIa.

It is difficult to establish the causes of the growth reductions within LETR-A. One possibility is that the damage was caused by bark beetles. Larvae feed under the bark of trees with low vitality and the adults emerging later feed on pine shoots, leading to a reduction in growth. The main defence of the trees, resin production, could have been hampered by low temperatures. However, the newly established woodland at the edge of its distribution range may have been sensitive to climatic changes in the transition from GI-1c to GI-1b and during the onset of the intra-Allerød cold period (13,311 b2K, Rasmussen et al., 2014). In the Netherlands, a substantial cooling also occurred around 13,2 ka cal yr BP, with much reduced precipitation and relatively dry conditions (Hoek and Bohncke, 2002). These cold intra-Allerød conditions may have helped to preserve the fallen trees of LETR-A in relatively damp conditions within the depression.

Compared to the commonly accepted dating of the second intra-Allerød arrival of *Pinus* in the Netherlands in c. 11,250 BP/c. 13,140 cal yr BP (*Pinus sylvestris* in the total pollen sum >20% (Hoek, 1997)), the younger LETR-B pines seem to have reached maturity relatively late. Although a cooling event (GI-1b) occurred at the time that pine arrived, this increase can perhaps be seen as the effect of a more continental climate (Hoek et al., 1999). The absence of (macroscopical parts of) cones at this site could be the result of prolonged degradation or predation by animals after the trees had died off, or could be evidence that the trees bore little or no fruit during the final stages of their lives due to their climatically marginal position. The demise of the group of *Pinus* trees of LETR-B within years or a few decades after c. 12,740 cal yr BP is contemporaneous with the dramatic *Pinus* pollen decline in Dutch pollen diagrams: this decline is generally interpreted as the result of a sudden disappearance of pine woodland at the start of the Younger Dryas. Northwestern Europe during GS-1 was ultimately characterized by short and/or low-temperature growing seasons incompatible with pine woodland growth. For the transition from the Allerød to the Younger Dryas period in the Netherlands, a decline in the average July temperature from 15 to 18° to 10–13° and of average January temperatures from −16 to 6° to −15 to −7° was established (Hoek and Bohncke, 2002). The average annual temperature fell to below −1°, and perhaps even down to −2 to −5°, giving rise to discontinuous permafrost (Isarin, 1997). Given the relatively narrow ring widths of LETR-B, the regular occurrence of (prolonged) stress and the possible lack of fruit bearing at the end of this forest phase, it is hypothesized that the pines constituting LETR-B suffered unfavourable regional growing conditions associated with the onset of the Younger Dryas (GS-1) event (Fig. 12): regeneration problems because of low summer temperatures and/or death because of snow cover extending into late spring, growing seasons that were too short and/or low effective temperature sums during the growing season.

6. Conclusions

During sand-extraction works at Leusden-Den Treek, the Netherlands, a waterlogged Usselo soil was documented. *In situ* subfossil pine woodland remains from the later part of the Bølling-Allerød interstadial (GI-1) were investigated. The tree-ring series show the occurrence of two successive phases of pine woodland development which have been ^{14}C dated and calibrated using the recent IntCal20 dataset: LETR-A (n = 16, 106 years) = c. 13,450–13,396 to 13,370–13,316 cal yr BP; and LETR-B (n = 24, 201 years) = 12,952–12,937 to 12,754–12,739 cal yr BP. Before c. 13,455 ± 25 cal yr BP, an open, dry landscape with a sparse vegetation cover became significantly wetter and/or more vegetated. Aeolian dust settled at the site within a herb-rich and open *Betula* woodland and a soil developed. At c. 13,455 ± 25 cal yr BP, during a relatively warm period (GI-1c), a mature *Betula* woodland was replaced by a *Pinus* woodland. As evidenced by tree-ring series LETR-A, this woodland existed for more than a century under relatively favourable and stable growing conditions. At the edge of its distribution range, however, *Pinus* was sensitive to climatic changes at the transition from GI-1c to GI-1b (13,311 b2K, Rasmussen et al., 2014) and the onset of the intra-Allerød cold period. It was impossible to disentangle in the field the oldest tree group (LETR-A) and the youngest (LETR-B) on the basis of stratigraphy, although there is a gap of about 400 years, contemporaneous with the relatively cold period GI-1b. The survival of vegetation impeded a substantial local deposition of sediment. The renewed establishment of *Pinus* at the site during the late Allerød is securely dated at c. 12,950 cal yr BP (tree-ring series LETR-B), halfway the relatively warm period GI-1a. The litter layer or A-horizon of the trees is well preserved. During the last phase of woodland development, more humid conditions prevailed. The start of the Younger Dryas (GS-1) was clearly revealed in all the Leusden data. The date of the inability to set fruit and the demise of the Allerød woodland at Leusden – some decades before and after c. 12,740 cal yr BP – is considered a precise indication of vegetational response to abrupt climate deterioration at the start of the Younger Dryas (12,807 ± 12 cal BP) (Reinig et al., 2021). This lag is important in understanding the relationship between shifts in sedimentation – indicating the sharp transition into the Younger Dryas - and the pollen signal in annually laminated lake sediments at the Allerød-Younger Dryas transition. Under cold climate conditions, (dwarf) birch (*Betula nana*) and a wide variety of herbs expanded during the early Younger Dryas, after the disappearance of the pine woodland. This coincided with wetter surface conditions. Subsequently, the landscape opened up considerably and *Empetrum* expanded at the expense of *Betula*, Poaceae and Cyperaceae under cooling climatic conditions and an increase in aeolian activity. Most or all vegetation eventually disappeared at the site, and substantial coversands were deposited.

Declaration of competing interest

The authors declare that they have no known competing financial interests or personal relationships that could have appeared to influence the work reported in this paper.

Acknowledgements

We would like to thank J.M.A. Diepenhorst, the *rentmeester* of the Den Treek-Henschoten estate, Jkvr. F. de Beaufort, member of the Board of Directors of the Den Treek-Henschoten estate, the estate manager M. Nolsen, and A. Buijtenhuis, the director of Buijtenhuis Nijkerk B.V., for their permission and their support for the field research in 2016–2017. The excavation would not have been possible without the mediation and support of M. van Heek of Eye and Image. Fieldwork was carried out by Willem Derickx, Menno van der Heiden, Mario van IJzendoorn, Wim Jong and Jan Willem de Kort (all Cultural Heritage Agency, Amersfoort). The dendrochronological research done by the Netherlands Centre for Dendrochronology/RING Foundation, Amersfoort, was funded by the Cultural Heritage Agency, Amersfoort, grant number MS2017-

236 (d.d. 1-12-2017). We benefited from discussions with Dr B. Kromer from Heidelberg University on the interpretation of the ^{14}C dates from Leusden-Den Treek. We thank Michael Friedrich for the opportunity to compare the dendrochronological data from Leusden with those from Warendorf, Reichwalde, the German Danube and Breithenthal. We would like to thank Annette Visser for her editing services and preparing the article for publication and Marjolein Haars for the artwork.

Appendix A. Supplementary data

Supplementary data to this article can be found online at https://doi.org/10.1016/j.quascirev.2021.107199. Dendrochronological data in Heidelberg format can be requested from the corresponding author.

References

Aerts-Bijma, A.T., Van der Plicht, J., Meijer, H.A.J., 2001. Automatic AMS sample combustion and CO_2 collection. Radiocarbon 43 (2), 293–298. https://doi.org/10.1017/S0033822200038133.

Anderson, R.F., Ali, S., Bradtmiller, L.I., Nielsen, S.H.H., Fleisher, M.Q., Anderson, B.E., Burckle, L.H., 2009. Wind-driven upwelling in the Southern Ocean and the deglacial rise in atmospheric CO2. Science 323, 1443–1448. https://doi.org/10.1126/science.1167441.

Arzac, A., Popkova, M., Anarbekova, A., Olano, J.M., Gutiérrez, E., Nikolaev, A., Shishov, V., 2019. Increasing radial and latewood growth rates of Larix cajanderi Mayr. and Pinus sylvestris L. in the continuous permafrost zone in Central Yakutia (Russia). Ann. For. Sci. 76, 96. https://doi.org/10.1007/s13595-019-0881-4.

Beug, H.-J., 2004. Leitfaden der Pollenbestimmung für Mitteleuropa und angrenzende Gebiete. Dr. Friedrich Pfeil, München.

Birks, H.H., Birks, H.J.B., 2014. To what extent did changes in July temperature influence Lateglacial vegetation patterns in NW Europe? Quat. Sci. Rev. 106, 262–277. https://doi.org/10.1016/j.quascirev.2014.06.024.

Bohncke, S.J.P., 1993. Lateglacial environmental changes in The Netherlands: spatial and temporal patterns: a contribution to the 'North Atlantic seaboard programme' of IGCP-253, 'Termination of the Pleistocene. Quat. Sci. Rev. 12, 707–717. https://doi.org/10.1016/0277-3791(93)90008-A.

Bos, J.A., Bohncke, S.J., Janssen, C.R., 2006. Lake-level fluctuations and small-scale vegetation patterns during the late glacial in The Netherlands. J. Paleolimnol. 35, 211–238.

Brauer, A., Haug, G.H., Dulski, P., Sigman, D.M., Negendank, J.F.W., 2008. An abrupt wind shift in western Europe at the onset of the Younger Dryas cold period. Nat. Geosci. 1, 520–523. https://doi.org/10.1038/ngeo263.

Bronk Ramsey, C., 2009. Bayesian analysis of radiocarbon dates. Radiocarbon 51, 337–360. https://doi.org/10.1017/S0033822200033865.

Burns, R.M., Honkala, B.H., 1990. Silvics of North America 1. Conifers. Agriculture Handbook, Washington.

Capano, M., Miramont, C., Guibal, F., Kromer, B., Tuna, T., Fagault, Y., Bard, E., 2018. Wood 14C dating with AixMICADAS: methods and application to tree-ring sequences from the younger Dryas event in the southern French alps. Radiocarbon 60, 51–74. https://doi.org/10.1017/RDC.2017.83.

Carlson, A., 2013. The younger Dryas climate event. Encyclopedia Quat. Sci. 3, 126–134. https://doi.org/10.1016/B978-0-444-53643-3.00029-7.

Cook, E., Briffa, K., Shiyatov, S., Mazepa, V., Jones, P.D., 1990. Data analysis. Methods of dendrochronology. Springer, pp. 97–162.

De Jong, J., 1979. Uitkomst van een C14 ouderdomsbepaling aan materiaal afkomstig uit een boring bij Achterberg. Rijksgeologische Dienst, Rapport 812a, Afdeling Palaeobotanie.

Dee, M.W., Palstra, S.W.L., Aerts-Bijma, A.T., Bleeker, M.O., De Bruijn, S., Ghebru, F., Jansen, H.G., Kuitems, M., Paul, D., Richie, R.R., Spriensma, J.J., Scifo, A., Zonneveld, D. van, Verstappen-Dumoulin, B.M.a.A., Wietzes-Land, P., Meijer, H.a.J., 2020. Radiocarbon dating at Groningen: new and updated chemical pretreatment procedures. Radiocarbon 62, 63–74. https://doi.org/10.1017/RDC.2019.101.

Dekker, L.W., Booij, A.H., Vroon, H.R.J., Koopman, G.J., 1991. Waterhardlagen: indicatoren van een voormalig veendek. Grondboor Hamer 45, 25–30.

Denton, G.H., Anderson, R.F., Toggweiler, J.R., Edwards, R.L., Schaefer, J.M., Putnam, A.E., 2010. The last glacial termination. Science 328, 1652–1656. https://doi.org/10.1126/science.1184119.

Dulamsuren, C., Hauck, M., Leuschner, C., 2013. Seedling emergence and establishment of Pinus sylvestris in the Mongolian forest-steppe ecotone. Plant Ecol. 214, 139–152. https://doi.org/10.1007/s11258-012-0152-z.

Dzieduszyńska, D.A., Kittel, P., Petera-Zganiacz, J., Brooks, S.J., Korzeń, K., Krąpiec, M., Pawłowski, D., Płaza, D.K., Płóciennik, M., Stachowicz-Rybka, R., Twardy, J., 2014. Environmental influence on forest development and decline in the Warta River valley (Central Poland) during the Late Weichselian. Quaternary International, Human dimensions of palaeoenvironmental change: Geomorphic processes and geoarchaeology 324, 99–114. https://doi.org/10.1016/j.quaint.2013.07.017.

Eckstein, D., Bauch, J., 1969. Beitrag zur Rationalisierung eines dendrochronologischen Verfahrens und zur Analyse seiner Aussagesicherheit. Forstwiss. Cent.blatt 88, 230–250. https://doi.org/10.1007/BF02741777.

Faegri, K., Iversen, J., Kaland, P.E., Krzywinski, K., 1989. Textbook of Pollen Analysis. Blackburn Press, Caldwell, New York.

Florschütz, F., 1941. Resultaten van microbotanisch onderzoek van het complex loodzand-oerzand en van daaronder en daarboven gelegen afzettingen. Besprekingen over het Heidepodsolprofiel 3–21.

Friedrich, M., Remmele, S., Kromer, B., Hofmann, J., Spurk, M., Kaiser, K.F., Orcel, C., Küppers, M., 2004. The 12,460-Year Hohenheim Oak and Pine Tree-Ring Chronology from Central Europe. A unique annual record for radiocarbon calibration and paleoenvironment reconstructions. Radiocarbon 46, 1111–1122. https://doi.org/10.1017/S003382220003304X.

Grace, J., Jarvis, P.G., Hutchings, N., Monteith, J.L., Shuttleworth, W.J., Fowler, D., Corlett, J., Thomas, J., Jarvis, Paul Gordon, Monteith, John Lennox, Shuttleworth, W.J., Unsworth, M.H., 1989. Tree lines. Philos. Trans. R. Soc. Lond. B Biol. Sci. 324, 233–245. https://doi.org/10.1098/rstb.1989.0046.

Grace, J., Norton, D.A., 1990. Climate and growth of Pinus sylvestris at its upper altitudinal limit in Scotland: evidence from tree growth-rings. J. Ecol. 78, 601–610. https://doi.org/10.2307/2260887.

Gregorich, E.G., Turchenek, L.W., Carter, M.R., Angers, D.A., 2001. Soil and Environmental Science Dictionary. CRC Press.

Heiri, O., Lotter, A.F., Lemcke, G., 2001. Loss on ignition as a method for estimating organic and carbonate content in sediments: reproducibility and comparability of results. J. Paleolimnol. 25, 101–110. https://doi.org/10.1023/A:1008119611481.

Hoek, W.Z., 2001. Vegetation response to the ~14.7 and ~11.5 ka cal. BP climate transitions: is vegetation lagging climate? Global Planet. Change 30, 103–115. https://doi.org/10.1016/S0921-8181(01)000.81-9.

Hijszeler, C.C.W.J., 1957. Late-Glacial human cultures in the Netherlands. Geologie en Mijnbouw 19, 203–288.

Hoek, W.Z., 1997. *Palaeogeography of Lateglacial Vegetations* (Urn:nbn:nl:ui:31-1871/12731). Vrije Universiteit, Amsterdam.

Hoek, W.Z., Bohncke, S.J.P., 2002. Climatic and environmental events over the Last Termination, as recorded in The Netherlands: a review. Neth. J. Geosci. 81, 123–137. https://doi.org/10.1017/S001677460002062X.

Hoek, W.Z., 2008. The Last Glacial-Interglacial Transition. Episodes 31 (2), 226–229. https://doi.org/10.18814/epiiugs/2008/v31i2/007.

Hoek, W.Z., Bohncke, S.J.P., 2001. Oxygen-isotope wiggle matching as a tool for synchronising ice-core and terrestrial records over Termination 1. Quat. Sci. Rev. 20, 1251–1264. https://doi.org/10.1016/S0277-3791(00)00150-5.

Hoek, W.Z., Bohncke, S.J.P., Ganssen, G.M., Meijer, T.O.M., 1999. Lateglacial environmental changes recorded in calcareous gyttja deposits at Gulickshof, southern Netherlands. Boreas 28, 416–432. https://doi.org/10.1111/j.1502-3885.1999.tb00230.x.

Hollstein, E., 1980. Mitteleuropäische Eichenchronologie. Verlag Phillipp von Zabern, Mainz.

Holmes, R., 1999. Users Manual for Program Cofecha by Laboratory of Tree-Ring Research. University of Arizona, Tucson, Arizona.

Houstan Durrant, T., de Rigo, D., Caudullo, G., 2016. Pinus sylvestris in Europe: distribution, habitat, usage and threats. In: San-Miguel-Ayanz, J., de Rigo, D., Caudullo, G., Houston Durrant, T., Mauri, A. (Eds.), European Atlas of Forest Tree Species. Tree species, pp. 132–133.

Isarin, R.F.B., 1997. Permafrost distribution and temperatures in Europe during the younger Dryas. Permafr. Periglac. Process. 8, 313–333. https://doi.org/10.1002/(SICI)1099-1530(199709)8:3<313::AID-PPP255>3.0.CO;2-E.

Jansma, E., 2020. Hydrological disasters in the NW-European Lowlands during the first millennium AD: a dendrochronological reconstruction. Neth. J. Geosci. 99. https://doi.org/10.1017/njg.2020.10.

Kaiser, K., Hilgers, A., Schlaak, N., Jankowski, M., Kühn, P., Bussemer, S., Przegiętka, K., 2009. Palaeopedological marker horizons in northern central Europe: characteristics of Lateglacial Usselo and Finow soils. Boreas 38, 591–609. https://doi.org/10.1111/j.1502-3885.2008.00076.x.

Kaiser, K., Oldorff, S., Breitbach, C., Kappler, C., Theuerkauf, M., Scharnweber, T., Schult, M., Küster, M., Engelhardt, C., Heinrich, I., Hupfer, M., Schwalbe, G., Kirschey, T., Bens, O., 2018. A submerged pine forest from the early Holocene in the Mecklenburg Lake District, northern Germany. Boreas 47, 910–925. https://doi.org/10.1111/bor.12314.

Kaiser, K.F., Friedrich, M., Miramont, C., Kromer, B., Sgier, M., Schaub, M., Boeren, I., Remmele, S., Talamo, S., Guibal, F., 2012. Challenging process to make the Lateglacial tree-ring chronologies from Europe absolute—an inventory. Quat. Sci. Rev. 36, 78–90. https://doi.org/10.1016/j.quascirev.2010.07.009.

Kasse, C., 2002. Sandy aeolian deposits and environments and their relation to

climate during the Last Glacial Maximum and Lateglacial in northwest and central Europe. Prog. Phys. Geogr. 26, 507–532. https://doi.org/10.1191/0309133302pp350ra.
Kasse, C., 1999. Late pleniglacial and late glacial aeolian phases in The Netherlands. In: Schirmer, W. (Ed.), Dunes and Fossil Soils. GeoArchaeoRhein, vol. 3, pp. 61–82, 3.
Kasse, C., Tebbens, L.A., Tump, M., Deeben, J., Derese, C., Grave, J.D., Vandenberghe, D., 2018. Late Glacial and Holocene aeolian deposition and soil formation in relation to the Late Palaeolithic Ahrensburg occupation, site Geldrop-A2, The Netherlands. Neth. J. Geosci. 97, 3–29. https://doi.org/10.1017/njg.2018.1.
Kasse, C., Vandenberghe, D., Corte, F.D., Haute, P.V.D., 2007. Late Weichselian fluvio-aeolian sands and coversands of the type locality Grubbenvorst (southern Netherlands): sedimentary environments, climate record and age. J. Quat. Sci. 22, 695–708. https://doi.org/10.1002/jqs.1087.
Kirchhefer, A.J., 2000. Dendroclimatology on Scots Pine (Pinus Sylvestris L.) in Northern Norway. University of Norway.
Knibbe, B., 2008. PAST4-Personal Analysis System for Treering Research Version 4.5. SCIEM, Vienna.
Knibbe, B., 2014. PAST5 - Personal Analysis System for Treering Research Software Version 5.0.575. SCIEM, Vienna.
Konert, M., Vandenberghe, J., 1997. Comparison of laser grain size analysis with pipette and sieve analysis: a solution for the underestimation of the clay fraction. Sedimentology 44, 523–535. https://doi.org/10.1046/j.1365-3091.1997.d01-38.x.
Konovalov, V.N., Zarubina, L.V., Goreva, A.D., 2019. Peculiar influence of nitrogen on the daily growth and photosynthesis of Scots Pine in the far north. Earth Environ. Sci. 263, 012011. https://doi.org/10.1088/1755-1315/263/1/012011.
Koopman, G., 1986. Waterhard: wat het is en wat-er-hard aan is . Een studie van het fenomeen “waterhard” in het Amsterdamsche Veld bij Erica (Drente). Faculty of Science and Engineering, Groningen.
Koopman, G.J., 1988. “Waterhard”: a hard brown layer in sand below peat, The Netherlands. Geoderma 42, 147–157. https://doi.org/10.1016/0016-7061(88)90030-4.
Lane, C.S., Brauer, A., Blockley, S.P.E., Dulski, P., 2013. Volcanic ash reveals time-transgressive abrupt climate change during the Younger Dryas. Geology 41, 1251–1254. https://doi.org/10.1130/G34867.1.
Lindholm, M., 1996. Reconstruction of Past Climate from Ring-Width Chronologies of Scots Pine (Pinus Sylvestris L.) at the Northern Forest Limit in Fennoscandia. University of Joensuu, Joensuu.
Lowe, J.J., Rasmussen, S.O., Björck, S., Hoek, W.Z., Steffensen, J.P., Walker, M.J.C., Yu, Z.C., 2008. Synchronisation of palaeoenvironmental events in the North Atlantic region during the Last Termination: a revised protocol recommended by the INTIMATE group. Quat. Sci. Rev. 27, 6–17. https://doi.org/10.1016/j.quascirev.2007.09.016.
Maarleveld, G.C., van der Schans, R.P.H.P., 1961. De dekzandmorfologie van de Gelderse Vallei. Tijdschrift Koninklijk Nederlands Aardrijkskundig Genootschap 78, 24–34.
Mangerud, J., 2021. The discovery of the Younger Dryas, and comments on the current meaning and usage of the term. Boreas 50, 1–5. https://doi.org/10.1111/bor.12481.
Mauquoy, D., Van Geel, B., 2007. Plant macrofossil methods and studies: Mire and peat macros. In: Elias, S.A. (Ed.), Encyclopedia of Quaternary Science, pp. 2315–2336. https://doi.org/10.1016/B0-44-452747-8/00229-5.
Mook, W.G., 2006. Introduction to Isotope Hydrology. Taylor & Francis, London etc.
Moreno, A., Svensson, A., Brooks, S.J., Connor, S., Engels, S., Fletcher, W., Genty, D., Heiri, O., Labuhn, I., Perşoiu, A., Peyron, O., Sadori, L., Valero-Garcés, B., Wulf, S., Zanchetta, G., 2014. A compilation of Western European terrestrial records 60–8 ka BP: towards an understanding of latitudinal climatic gradients. Quat. Sci. Rev. 106, 167–185. https://doi.org/10.1016/j.quascirev.2014.06.030.
Nijland, T.G., Zwaan, J.C., Visser, D., Leloux, J., 2007. Geologie Van Nederland. *De mineralen van Nederland*. Naturalis, Leiden.
Nikolov, N., Helmisaari, H., 1992. Silvics of the circumpolar boreal forest tree species. In: Bonan, G.B., Shugart, H.H., Leemans, R. (Eds.), A Systems Analysis of the Global Boreal Forest. Cambridge University Press, Cambridge, pp. 13–84. https://doi.org/10.1017/CBO9780511565489.003.
Pauly, M., Helle, G., Büntgen, U., Wacker, L., Treydte, K., Reinig, F., Turney, C., Nievergelt, D., Kromer, B., Friedrich, M., Sookdeo, A., Heinrich, I., Riedel, F., Balting, D., Brauer, A., 2020. An annual-resolution stable isotope record from Swiss subfossil pine trees growing in the late Glacial. Quat. Sci. Rev. 247, 106550. https://doi.org/10.1016/j.quascirev.2020.106550.
Perks, W.A.G., 1984. Den Treek: Van Marke Tot Landgoed, 2e ed. Bekking, Amersfoort.
Polak, B., 1963. A buried Allerød pine-forest. Acta Bot. Neerl. 12, 533–538.
Prentice, C.I., Helmisaari, H., 1991. Silvics of north European trees: compilation, comparisons and implications for forest succession modelling. Forest Ecology and Management, Modelling Forest Succession in Europe 42, 79–93. https://doi.org/10.1016/0378-1127(91)90066-5.
Rasmussen, S.O., Andersen, K.K., Svensson, A.M., Steffensen, J.P., Vinther, B.M., Clausen, H.B., Siggaard-Andersen, M.-L., Johnsen, S.J., Larsen, L.B., Dahl-Jensen, D., Bigler, M., Röthlisberger, R., Fischer, H., Goto-Azuma, K., Hansson, M.E., Ruth, U., 2006. A new Greenland ice core chronology for the last glacial termination. J. Geophys. Res.: Atmospheres 111. https://doi.org/10.1029/2005JD006079.
Rasmussen, S.O., Bigler, M., Blockley, S.P., Blunier, T., Buchardt, S.L., Clausen, H.B., Cvijanovic, I., Dahl-Jensen, D., Johnsen, S.J., Fischer, H., Gkinis, V., Guillevic, M., Hoek, W.Z., Lowe, J.J., Pedro, J.B., Popp, T., Seierstad, I.K., Steffensen, J.P., Svensson, A.M., Vallelonga, P., Vinther, B.M., Walker, M.J.C., Wheatley, J.J., Winstrup, M., 2014. A stratigraphic framework for abrupt climatic changes during the Last Glacial period based on three synchronized Greenland ice-core records: refining and extending the INTIMATE event stratigraphy. Quat. Sci. Rev. 106, 14–28. https://doi.org/10.1016/j.quascirev.2014.09.007.
Rea, B.R., Pellitero, R., Spagnolo, M., Hughes, P., Ivy-Ochs, S., Renssen, H., Ribolini, A., Bakke, J., Lukas, S., Braithwaite, R.J., 2020. Atmospheric circulation over Europe during the younger Dryas. Sci. Adv. 6, eaba4844. https://doi.org/10.1126/sciadv.aba4844.
Reimer, P.J., Austin, W.E.N., Bard, E., Bayliss, A., Blackwell, P.G., Ramsey, C.B., Butzin, M., Cheng, H., Edwards, R.L., Friedrich, M., Grootes, P.M., Guilderson, T.P., Hajdas, I., Heaton, T.J., Hogg, A.G., Hughen, K.A., Kromer, B., Manning, S.W., Muscheler, R., Palmer, J.G., Pearson, C., Plicht, J. van der, Reimer, R.W., Richards, D.A., Scott, E.M., Southon, J.R., Turney, C.S.M., Wacker, L., Adolphi, F., Büntgen, U., Capano, M., Fahrni, S.M., Fogtmann-Schulz, A., Friedrich, R., Köhler, P., Kudsk, S., Miyake, F., Olsen, J., Reinig, F., Sakamoto, M., Sookdeo, A., Talamo, S., 2020. The IntCal20 northern hemisphere radiocarbon age calibration curve (0–55 cal kBP). Radiocarbon 62, 725–757. https://doi.org/10.1017/RDC.2020.41.
Reinig, F., Nievergelt, D., Esper, J., Friedrich, M., Helle, G., Hellmann, L., Kromer, B., Morganti, S., Pauly, M., Sookdeo, A., Tegel, W., Treydte, K., Verstege, A., Wacker, L., Büntgen, U., 2018. New tree-ring evidence for the Late Glacial period from the northern pre-Alps in eastern Switzerland. Quat. Sci. Rev. 186, 215–224. https://doi.org/10.1016/j.quascirev.2018.02.019.
Reinig, F., Sookdeo, A., Esper, J., Friedrich, M., Guidobaldi, G., Helle, G., Kromer, B., Nievergelt, D., Pauly, M., Tegel, W., Treydte, K., Wacker, L., Büntgen, U., 2020. Illuminating intcal during the younger Dryas. Radiocarbon 62, 883–889. https://doi.org/10.1017/RDC.2020.15.
Reinig, F., Wacker, L., Jöris, O., Oppenheimer, C., Guidobaldi, G., Nievergelt, D., Adolphi, F., Cherubini, P., Engels, S., Esper, J., Land, A., Lane, C., Pfanz, H., Remmele, S., Sigl, M., Sookdeo, A., Büntgen, U., 2021. Precise date for the laacher see eruption synchronizes the younger Dryas. Nature 595, 66–69. https://doi.org/10.1038/s41586-021-03608-x.
Renssen, H., 2020. Comparison of climate model simulations of the younger Dryas cold event. Quaternary 3, 29. https://doi.org/10.3390/quat3040029.
Renssen, H., Isarin, R.F.B., 2001. The two major warming phases of the last deglaciation at ~14.7 and ~11.5 ka cal BP in Europe: climate reconstructions and AGCM experiments. Global Planet. Change 30, 117–153. https://doi.org/10.1016/S0921-8181(01)00082-0.
Schibalski, A., Lehtonen, A., Schröder, B., 2014. Climate change shifts environmental space and limits transferability of treeline models. Ecography 37, 321–335. https://doi.org/10.1111/j.1600-0587.2013.00368.x.
Schokker, J., Weerts, H.J.T., Westerhoff, W.E., Berendsen, H.J.A., Den Otter, C., 2007. Introduction of the Boxtel Formation and implications for the quaternary lithostratigraphy of The Netherlands. Neth. J. Geosci. 86, 197–210.
Schweingruber, F.H., Eckstein, D., Serre-Bachet, F., Bräker, O.U., 1990. Identification, presentation and interpretation of event years and pointer years in dendrochronology. Dendrochronologia 8, 9–38.
Steffensen, J.P., Andersen, K.K., Bigler, M.M., Clausen, H.B., Dahl-Jensen, D., Fischer, H., Goto-Azuma, K., Hansson, M., Johnson, S.J., Jouzel, J., Masson-Delmotte, V., Popp, T., Rasmussen, S.O., Röthlisberger, R., Ruth, U., Stauffer, B., Siggaard-Andersen, M.-L., Sveinbjörnsdottir, A.E., Svensson, A.M., White, J.W.C., et al., 2008. High-Resolution Greenland Ice Core Data Show Abrupt Climate Change Happens in Few Years. Science 5889, 680–684. https://doi.org/10.1126/science.1157707.
Synal, H.-A., Stocker, M., Suter, M., 2007. MICADAS: A new compact radiocarbon AMS system. Nuclear Instruments and Methods in Physics Research, Section B: Beam Interactions with Materials and Atoms 259 (1), 7–13. https://doi.org/10.1016/j.nimb.2007.01.138.
Tchebakova, N.M., Parfenova, E., Soja, A.J., 2009. The effects of climate, permafrost and fire on vegetation change in Siberia in a changing climate. Environ. Res. Lett. 4, 045013. https://doi.org/10.1088/1748-9326/4/4/045013.
Toggweiler, J.R., 2009. Climate change. Shifting westerlies. Science 323, 1434–1435. https://doi.org/10.1126/science.1169823.
Tuovinen, M., 2005. Response of tree-ring width and density of Pinus sylvestris to climate beyond the continuous northern forest line in Finland. Dendrochronologia 22, 83–91. https://doi.org/10.1016/j.dendro.2005.02.001.
Van Asch, N., Heiri, O., Bohncke, S.J., Hoek, W.Z., 2013. Climatic and environmental changes during the weichselian lateglacial interstadial in the weerterbos region, The Netherlands. Boreas 42, 123–139. https://doi.org/10.1111/j.1502-3885.2012.00281.x.
Van Balen, R.T., Bakker, M.A.J., Kasse, C., Wallinga, J., Woolderink, H.A.G., 2019. A late glacial surface rupturing earthquake at the peel boundary fault zone, roer valley

rift System, The Netherlands. Quat. Sci. Rev. 218, 254–266. https://doi.org/10.1016/j.quascirev.2019.06.033.
Van der Hammen, T., 1951. Late-glacial flora and periglacial phenomena in The Netherlands. Leidse Geol. Meded. 17, 71–183.
Van der Plicht, J., Hogg, A., 2006. A note on reporting radiocarbon. Quat. Geochronol. 1, 237–240. https://doi.org/10.1016/j.quageo.2006.07.001.
Van Dijk, D., Houba, V.J.G., 2000. Homogeneity and stability of materials distributed within the Wageningen evaluating programmes for analytical laboratories. Commun. Soil Sci. Plant Anal. 31, 1745–1756. https://doi.org/10.1080/00103620009370534.
Van Geel, B., Brinkkemper, O., van Reenen, G.B.A., Van der Putten, N.N.L., Sybenga, J.E., Soonius, C., Kooijman, A.M., Hakbijl, T., Gosling, W.D., 2020. Multicore study of upper Holocene Mire development in west-frisia, northern Netherlands: Ecological and archaeological aspects. Quaternary 3, 12. https://doi.org/10.3390/quat3020012.
Van Geel, B., Coope, G.R., Van der Hammen, T., 1989. Palaeoecology and stratigraphy of the lateglacial type section at Usselo (The Netherlands). Rev. Palaeobot. Palynol. 60, 25–129. https://doi.org/10.1016/0034-6667(89)90072-9.
Van Hateren, J.A., Van Buuren, U., Arens, S.M., Van Balen, R.T., Prins, M.A., 2020. Identifying sediment transport mechanisms from grain size–shape distributions, applied to aeolian sediments. Earth Surface Dynamics 8, 527–553. https://doi.org/10.5194/esurf-8-527-2020.
Van Heuveln, B., De Bakker, H., 1972. Soil-forming processes in Dutch peat soils with special reference to humus-illuviation. Proceedings of the 4th International Peat Congress I-IV 289–297.
Van Hoesel, A., Hoek, W.Z., Braadbaart, F., Van der Plicht, J., Pennock, G.M., Drury, M.R., 2012. Nanodiamonds and wildfire evidence in the Usselo horizon postdate the Allerød-Younger Dryas boundary. Proc. Natl. Acad. Sci. Unit. States Am. 109, 7648–7653. https://doi.org/10.1073/pnas.1120950109.
Van Mourik, J.M., Slotboom, R.T., 1995. The expression of the tripartition of the Allerod chronozone in the lithofacies of late Glacial polycyclic profiles in Belgium and The Netherlands. Meded. Rijks Geol. Dienst 52, 441–450.
Vandenberghe, D.A.G., Derese, C., Kasse, C., Van den haute, P., 2013. Late Weichselian (fluvio-)aeolian sediments and Holocene drift-sands of the classic type locality in Twente (E Netherlands): a high-resolution dating study using optically stimulated luminescence. Quat. Sci. Rev. 68, 96–113. https://doi.org/10.1016/j.quascirev.2013.02.009.
Vandenberghe, J., Coope, R., Kasse, C., 1998. Quantitative reconstructions of palaeoclimates during the last interglacial–glacial in western and central Europe: an introduction. J. Quat. Sci. 13, 361–366. https://doi.org/10.1002/(SICI)1099-1417(1998090)13:5<361::AID-JQS404>3.0.CO;2-O.
Westerink, R.M., 1981. Geologie en geomorfologie van stuwwal, gordeldekzand en Gelderse vallei ten zuiden van Amersfoort (Amsterdam).